Elsevier Editorial System(tm) for Sensors & Actuators: B. Chemical

Manuscript Draft

Manuscript Number: SNB-D-16-03158

Title: ELEMENTAL MERCURY VAPOUR CHEMORESISTORS EMPLOYING TIO2 NANOFIBRES PHOTOCATALYTICALLY DECORATED WITH AU-NANOPARTICLES

Article Type: VSI: EUROSENSORS 2015

Section/Category: General section

Keywords: Hybrid conductive sensor, titania nanofibres, photocatalysis, gold nanoparticles, elemental mercury detection

Corresponding Author: Dr. Antonella Macagnano,

Corresponding Author's Institution: Institute of Atmospheric Pollution Research

First Author: Antonella Macagnano

Order of Authors: Antonella Macagnano; Viviana Perri; Emiliano Zampetti; Anna Ferretti; Francesca Sprovieri; Nicola Pirrone; Andrea Bearzotti; Fabrizio De Cesare

Abstract: The complex cycle of mercury in the environment together with its toxicity, explains the need to involve both local and global actions to develop detection and monitoring systems characterised by fast responses, low cost, low maintenance and ease of use. As a result of the combination of gold affinity for mercury with the nanoscale size of the frameworks, gold nanostructures look the most promising nanomaterials for creating novel sensors with sensing features comparable to those of commercial complex and expensive analytical systems currently available. Composite nanofibrous electrospun layers of titania decorated with gold nanoparticles (AuNPs) were fabricated to obtain nanostructured materials capable of adsorbing elemental mercury. Linker-free gold nanoparticles were grown on the electrospun titania nanofibres through the photocatalytic reduction of tetrachloroauric acid carried out by UV-irradiated nanofibres of titania in the presence of an organic capping reagent. Chemoresistors employing such decorated nanomaterials were then created in order to detect mercury vapours in the atmosphere. Various decorations of titania nanofibres with gold nanoparticles after deposition onto distinct substrates were morphologically investigated at nanoscale. The electrical properties of the resulting chemoresistors were measured. The capacity of chemoresistors employing various amounts of AuNPs for detecting low concentrations of mercury vapours (tens of ppt) in both static and dynamic (i.e. under a carrier gas flow - synthetic air) conditions was tested. The potential of the resulting sensors in environmental monitoring of elemental mercury vapours is discussed.

Suggested Reviewers: Krishna Persaud
krishna.persaud@manchester.ac.uk

Tamer Uyar
tamer@unam.bilkent.edu.tr

Eyal Zussman
meeyal@tx.technion.ac.il

Seeram Ramakrishna
seeram@nus.edu.sg

Jose Maria Lagaron
lagaron@iata.csic.es

Cover Letter

Revised version of the manuscript submitted to the EUROSENSORS 2015 Virtual Issue (OLD NUMBER SNB-D-15-03825R2)

Title

ELEMENTAL MERCURY VAPOUR CHEMORESISTORS EMPLOYING TIO2 NANOFIBRES PHOTOCATALYTICALLY DECORATED WITH AU-NANOPARTICLES

Authors

A. Macagnano[1], V. Perri[2], E. Zampetti[1], A. Bearzotti[1], A.M. Ferretti[4], F. Sprovieri[3], N. Pirrone[1], F. De Cesare[5]

Affiliations

[1]Institute of Atmospheric Pollution Research – National Research Council (IIA-CNR), Monterotondo (RM), Via Salaria km 29, 300, 00016, Italy

[2] University of Calabria, via Pietro Bucci Arcavacata di Rende (CS), 87036, Italy

[3] Institute of Atmospheric Pollution Research – National Research Council, Arcavacata di Rende (CS), 87036, Italy

[4] Institute of Molecular Science and Technologies- National Research Council (ISTM-CNR), via G. Fantoli 16/15 Milano, I-20138, Italy

[5] University of Tuscia, Via S. Camillo de Lellis, Viterbo, 01100 Italy

Corresponding Author emails: a.macagnano@iia.cnr.it; antonella.macagnano@cnr.it

Graphical Abstract (for review)

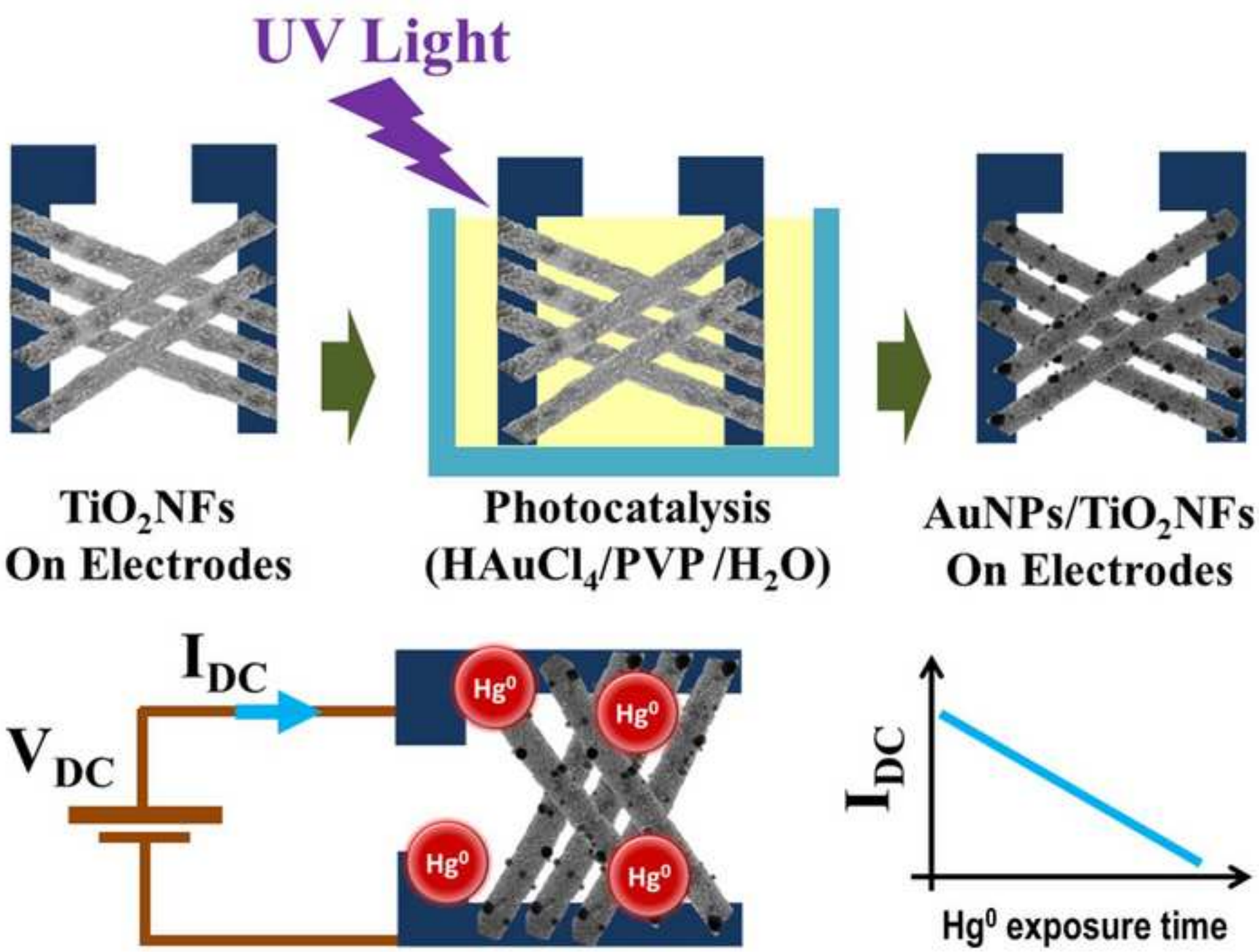

RESEARCH HIGHLIGHTS

- ✓ Electrospinning is a simple, continuous and scalable technique to fabricate metal oxide nanofibers with high-aspect ratio and controlled morphologies.
- ✓ Photocatalytic features of titania nanofibres can be exploited to grow gold nanoparticles selectively onto the fibrous scaffold: AuNPs are tunable in number and size through the fibres.
- ✓ The hybrid structure TiO_2/AuNPs is conductive at room temperature and it is able to detect elemental mercury in air at very low concentration

Title

ELEMENTAL MERCURY VAPOUR CHEMORESISTORS EMPLOYING TIO2 NANOFIBRES PHOTOCATALYTICALLY DECORATED WITH AU-NANOPARTICLES

Authors

A. Macagnano[1], V. Perri[2], E. Zampetti[1], A. Bearzotti[1], A.M. Ferretti[4], F. Sprovieri[3], G. Esposito[1], N. Pirrone[1], F. De Cesare[5]

Corresponding Author emails: *a.macagnano@iia.cnr.it; antonella.macagnano@cnr.it*

Abstract

The complex cycle of mercury in the environment together with its toxicity, explains the need to involve both local and global actions to develop detection and monitoring systems characterised by fast responses, low cost, low maintenance and ease of use. As a result of the combination of gold affinity for mercury with the nanoscale size of the frameworks, gold nanostructures look the most promising nanomaterials for creating novel sensors with sensing features comparable to those of commercial complex and expensive analytical systems currently available. Composite nanofibrous electrospun layers of titania decorated with gold nanoparticles (AuNPs) were fabricated to obtain nanostructured materials capable of adsorbing elemental mercury. Linker-free gold nanoparticles were grown on the electrospun titania nanofibres through the photocatalytic reduction of tetrachloroauric acid carried out by UV-irradiated nanofibres of titania in the presence of an organic capping reagent. Chemoresistors employing such decorated nanomaterials were then created in order to detect mercury vapours in the atmosphere. Various decorations of titania nanofibres with gold nanoparticles after deposition onto distinct substrates were morphologically investigated at nanoscale. The electrical properties of the resulting chemoresistors were measured. The capacity of chemoresistors employing various amounts of AuNPs for detecting low concentrations of mercury vapours (tens of ppt) in both static and dynamic (i.e. under a carrier gas flow - synthetic air) conditions was tested. The potential of the resulting sensors in environmental monitoring of elemental mercury vapours is discussed.

1. Introduction

Mercury is an element ubiquitous on the earth, and it is commonly released from natural sources (volcanoes, geothermal activity, wildfire and rock weathering) as well as human activities, such as metal production, gold extraction, manufacturing of chemicals, cement production, waste incineration, artisanal mining and fossil fuel combustion for electric power. Due to anthropogenic sources, the concentration of mercury in the environment has increased **[1-3]**. There is a great concern about such rise, since mercury has been linked to a variety of harmful effects on human health **[4]**. Historical reports on ancient civilisations, such as the Egyptians, the Romans, and the Chinese, have often suggested mercury compounds in cosmetics and medicines as a cause of death **[5]**. More recently, environmental disasters such as the spill of mercury released from a chemical plant in Minamata Bay (Japan, 1956-1968) and that consequent to the use of fungicides containing methylmercury (Iraq 1971) **[6,7]** renewed the global concern on the use and management of mercury and mercury products and pointed out the need to adopt major restrictions about mercury release. Recently, mercury has also been recognised as a pollutant producing significant adverse neurological damages, upon its action as a neurotoxin, as well as harmful effects on unborn children and infants. The most common way people are exposed to any form of mercury is by eating fish containing methylmercury (ingestion). Other possible ways of exposures include contact with breaking products containing elemental mercury and employing compounds that contain mercury (dermal contact) or breathing polluted air (inhalation). National Institute for Occupational Safety & Health (NIOSH) set a mercury Recommended Exposure Limit (REL) to 0.05 mg/m^3 for up to a 10 hour workday **[48]**. The level of Hg in air varies from 0.5ng/m^3 to 10 mg/m^3. The global release, transport and fate of mercury in the environment were the key reasons for taking the decision that a global action to address the problem of mercury pollution was required **[8,9,14,45,46]**. Since 2010, a European program called Global Mercury Observation System (GMOS) has been financed to create an international network capable of providing accurate measurements of Hg on a global scale **[47]**. In 2013, this European action became part of a world treaty called Minamata Convention on Mercury, assisted by UNEP and signed by 128 countries, with the dual aim to protect human health and the environment from anthropogenic emissions and to control and measure the release of mercury and mercury compounds in air.

In our planet, the mercury cycle is complex: it is emitted as both elemental and ionic forms. The former is fairly stable in the atmosphere (for some years) and travels for a range of distances **[10]**. About 95 percent of atmospheric mercury is elemental. Until now, the commercial monitoring systems for mercury detection in the atmosphere are highly sensitive and capable of detecting the

global mercury background. However, they are complex, time consuming sample preparation and pre-concentration procedures, expensive, often bulky equipment, high-maintenance instruments and require skilled operators, thus limiting their practical application for large areas monitoring and the most inaccessible areas of the planet. They mostly are capable of detecting mercury based on the spectroscopic features of this element. They employ, for example, atomic absorption spectroscopy (AAS), atomic fluorescence spectroscopy (AFS), atomic emission spectroscopy (AES), or mass spectrometry (MS) **[11,12]**. These instruments often include a series of processes or pre-treatments, such as oxidation, reduction, vapour separation and gold traps, to pre-concentrate and detect mercury from air. Additionally, an argon carrier stream is required by the detector to avoid the quenching of the fluorescence signal by oxygen, when fluorescence is the way of detection **[13]**.

The need for detection systems characterised by fast measurements, low costs, low-maintenance, wide distribution, ease of use, and resistance to adverse environmental conditions is becoming more and more urgent. Sensors and sensing systems are the most promising alternative to the traditional instruments, described herein above, and capable of satisfying the requirements. Many sensors have been designed and investigated to detect the several forms of mercury. Most of them have exploited the strong affinity between mercury and gold. Several studies have documented changes in the electrical properties, work function, and resistance of thin gold films upon exposure to various concentration of mercury vapour. Ignoring any effects of the carrier gas, the rate of adsorption from a single component vapor phase (k_{ads}) can be explained by considering the sticking probability (*S*), that is the rate at which atoms of the Hg^0 strike the surface (*v*), ($S=k_{ads}/\nu$). The parameter *S* depends on the adsorbate (Hg^0 in this case), its partial pressure (P_{Hg}), the substrate (Au), and the temperature (T).The sticking probability for mercury is close to unity on a clean gold surface in vacuum, but it decreases rapidly when more than 50% of gold surface is covered with mercury. This value is furtherly decreased when an inert gas, like argon, was introduced as gas carrier (by approximately 4 order of magnitude) [**15].** Vibrating micro-cantilevers have been employed, for example, to detect mercury by simply measuring the change of resonance frequency after adsorption of Hg^0 onto the surface of thin gold films **[16]**. Laboratory tests reported that the sensor sensitivity was depending on the exposed area: a larger surface allowed a greater mercury atoms adsorption over the same time and at the same vapour pressure. Real applications could be supposed by using an array of cantilevers differently sized in order to be able to work in different ranges of mercury concentration. However they had to work under dust-

free gas carrier and needed to be regeneration by heating (350 °C for 20 min). The mercury adsorption on a gold coated silicon wafer was also detected by measuring the changes in its surface acoustic waves (SAW devices) **[17,18]**. Flowing dry N_2 containing increasing concentration of mercury (ppb) for 30 min reported that the sensitivity was depending on the temperature (0.7 ppbv and 4.5 ppbv at 35°C and 55°C, respectively). Two hours occurred for completely desorbing the analyte. Quartz crystal microbalances (QCMs) could also provide mercury detection due to mercury adsorption onto their gold electrodes and related changes in their oscillation frequency **[19]**. These devices have been the first ones used as Hg vapor sensors in 1974 **[20]** and their sensing performances have been improved modulating the roughness of the pads. The QCM based Hg^0 vapor sensors were found to be highly portable and selective and they didn't require sample pretreatment making them highly suitable for online monitoring of Hg^0 vapor within industrial applications. More recent literature reported that electrodes having rougher surface showed higher Hg^0 absorptive capacity (700 ng cm^{-2}) than polished ones and a low limit of detection (LOD: 2.5 ppbv **[21]**). However the indicated 30-minute Hg^0 vapor exposure and 90-minute recovery periods necessary to achieve the highest response magnitudes and recovery efficiency from the sensor, suggested their limited use in real applications. Various conductometric devices used the adsorption of mercury vapour onto gold film to drive a change in their electrical resistance **[22,23]**. However the sensitivity of the latter group of sensors seemed often limited (around 1 μg/m^3). The employment of gold nanostructures (particles, wires, rods) has provided the chance to create more sensitive sensors, overall exploiting the optical properties of these nanostructures, mostly absorbance **[24]** and plasmonics (LSPR) **[25,26]**. Furthermore nanostructured electrochemical sensors **[27-29]**, gravimetric sensors **[30]** and conductometric sensors **[31]** have been investigated. The size and the shape of these nanostructures have been demonstrated to be key parameters in defining the properties of the resulting sensors, because of the strict relationship between the surface and the bulk of the sensing materials, that here is extremely reduced **[32]**. Thus, the electrochemical growth of gold-nanoprisms on QCM electrodes provided LODs of 2.4 ppbv (28°C) and 17 ppbv (89°C) making them potentially useful for monitoring the efficiency of Hg emission control systems in industries such as mining and waste incineration, exhibiting a sensor recovery within 1 h. It was also observed that these sensors based on gold, were highly selectivity to Hg vapor in the presence of ethanol, ammonia and humidity, and showed excellent long-term stability over a 33 day operating period. The increase in the number of binding sites, as well as the reduction of the time for mass transfer confirmed to be a successful strategies. Additional

parameters such as energy binding, surface adsorption kinetics and the diffusion rate of mercury into the nanogold structures have been widely investigated for designing novel sensors **[32]**. For instance, conductometric sensors based on CNTs finely decorated with AuNPs showed a strong dependence between the sensor response values and the number of gold nanoparticles. However, despite their high sensitivity (LOD: 2 ppbv) these sensors showed saturation at very low concentration (30 ppbv) **[33]**. In the present study, electrospinning technology **[34]** was used to create nanocomposite nanofibrous layers of Au/TiO_2 to employ in designing chemoresistors capable of adsorbing and revealing elemental mercury vapours in the atmosphere. In fact, from recent literature, electrospinning has been confirmed to be one of the most promising candidates among the various nanotechnologies for designing and developing smart and ultra-sensitive sensing systems, both for the uniqueness of the resulting nanostructures and for production rate and cost. Parameters like the extremely quick formation of the nanofibrous structures, which occurs on a millisecond scale, the easy tuning of shape and size, the large coverage in continuous mode and the nanofibres assembling in situ have raised great scientific and industrial interest. Since electrospinning is a technique capable of continuously creating fibres, i.e. with no interruption during the process, it sounds appropriate for the production of huge quantities of nanofibres, then also potentially attractive to the sensor market. By exploiting the photocatalytic properties of the nanofibres of titania, gold nanoparticles were selectively grown, under UV-light irradiation, on a nanofibrous scaffold of titania, using tetrachloroauric acid ($HAuCl_4$) as gold nanoparticles (AuNPs) precursor and polyvinylpyrrolidone (PVP) as organic capping reagent **[35]**. The resulting mercury adsorbent material was expected to be suitable for novel mercury sensors fabrication, since a similar nanofibrous scaffold doped with AuNPs was described in literature as filtering systems capable of adsorbing and removal mercury vapour from the environment with an efficiency of about 100% **[36]**. Additionally, the proposed method of functionalisation should provide also a chance of tuning the distribution and the size of the metal nanoparticles on the fibres. As a consequence, the possible resulting sensors could be conductive also at room temperature, due to the charge transfer among the neighbouring nanoparticles under a potential application. Micro-interdigitated electrodes (IDEs) of Pt/Ti were designed in order to create 3D-nanostructured chemoresistors potentially capable of adsorbing and revealing elemental mercury vapours in the atmosphere. As preliminary study, diverse non-woven nanofibrous layers of titania variously decorated with AuNPs were investigated in morphological and electrical properties. Chemoresistors were tested for their capacity of detecting Hg^0 vapours at room temperature.

Then, properly selected chemoresistors were used to detect low concentrations of mercury vapours (tens of ppt) in both static conditions and under a carrier gas (synthetic air) flow.

2. Materials and Methods

2.1. Chemicals

All chemicals were purchased from Sigma-Aldrich: polyvinylpyrrolidone (PVP, Mn 1,300,000), titanium isopropoxide (TiiP, d:0.96 g/mL), hydrogen tetrachloroaurate(III) hydrate ($HAuCl_4$, 99.9%), anhydrous ethanol ($EtOH_a$) and glacial acetic acid ($AcAc_g$). Ultrapure water ($5{\cdot}5\ 10^{-8}$ S cm^{-1}) was produced by MilliQ-EMD Millipore.

2.2. Electrospinning: solution and deposition

Electrospinning solution was prepared as follows: PVP was first dissolved in $EtOH_a$ (102.4 mg mL^{-1}) while stirring for at least 2 h. The TiiP solution (0.25 g mL^{-1}) solved in a mixture of $AcAc_g$ and $EtOH_a$ (1:1, v:v) was freshly prepared and added to the PVP solution under stirring (clear yellow final solution) for 1 h **[37]**. Both mixtures were prepared in a glove box under low humidity rate (<7% RH). The syringe filled with the TiiP/PVP solution was housed in a syringe pump (KDS 200, KD Scientific) working horizontally and set perpendicular to a 15 cm far grounded rotating cylindrical collector (45 mm diameter). The electrospinning apparatus used in the present study was designed and assembled in CNR laboratories (Rome, Italy) and the depositions were carried out in a home-made clean box equipped with temperature and humidity sensors. The syringe needle tip was connected to a positive DC-voltage (6 kV), with a feed rate of 150 ml h^{-1}. Two substrates were used for deposition: oxidised silicon wafers and interdigitated electrodes (IDEs). The substrates were fixed through suitable holders onto the collector (600 rpm, 21 °C and 35% RH) and processed for 20 min to obtain scaffolds for sensors and for 1 h to get a thicker fabric. After deposition, PVP/TiO_2 composite nanofibres were left for some hours at room temperature to undergo fully self-hydrolysis of TiiP **[38]**. Fibres annealing occurred under oxygen atmosphere (muffle furnace) using a thermal ramp from room temperature up to 550 °C (1 °C min^{-1}, 4 h dwell time) in order to remove PVP and crystallise the metal oxide (*anatase*).

2.3 AuNPs decoration of TiO_2 nanofibres

The resulting fibrous layers were immersed into two aqueous solutions containing $HAuCl_4$ differently diluted (called [α]=2.9 10^{-4} M and [β]=7.4 10^{-4} M) and PVP (0.1 M) as capping agent. Then, the substrates were exposed to UV-light irradiation for fixed periods to induce TiO_2 mediated catalytic Au oxidation onto TiO_2 nanofibres and formation of AuNPs/TiO_2 eletrospun nanofibrous scaffold. An UV lamp (365 nm) (Helios Italquartz) was used as UV light source. After UV irradiation, samples were rinsed extensively with water and then air-dried. Before morphological, electrical and sensing measurements, samples were heated at 450 °C per 1 h to remove completely the capping agent.

2.4 Fibres Characterisation

Samples deposited on silicon wafers were investigated by scanning electron microscopy (SEM), atomic force microscopy (AFM) and transmission electron microscopy (Conventional- and High Resolution-TEM (CT and HRT, respectively)). SEM micrographs were captured at 5 kV accelerating voltage (Jeol, JSM 5200, 20keV). AFM micrographs were captured in tapping mode using 190Al-G tips, 190 kHz, 48N/m (Nanosurf FlexAFM). CT and HRT micrographs were performed at 200 keV with an analytical double tilt probe (α ± 30°; β ± 15°) (ZEISS LIBRA 200FE HR-TEM). TEM specimen were prepared by gently scraping at first the TiO_2 nanofibrous layer electrospun onto the silicon support and then collecting the nanofibres through adhesion upon contact with holy carbon thin film **[39]**. SEM analyses of coatings electrospun onto IDEs were also used to assess the pattern (distribution, orientation, extent of coating and adhesion) of the electrospun fibres on the electrodes. The diameter size distribution of Au nanoparticles was evaluated through observation and statistical analysis of more than 150 nanoparticles (NPs). Images were analysed by means of iTEM (TEM Imaging Platform software by Olympus).

2.5. Electrical measurements

A single chemosensor, composed of a transducer coated with an AuNPs/TiO_2 eletrospun nanofibrous scaffold, was placed in a teflon measuring chamber. An electrometer (Keithley 6517) was used to measure the current (DC) through the device under test and transmit data to PC. Interdigitated electrodes (IDEs), composed of 40 pairs of Pt electrodes (150 nm thick, 20 μm width electrode, 20 μm gap) designed and manufactured in CNR (Italy) on oxidised silicon wafer, were used as transducers.

221 *2.6. Hg^0 vapour measurements*

222 In order to test the responsiveness of the device to low Hg^0 vapour concentrations, a procedure
223 was used employing an Hg^0 vapours delivery system, comprised of an Hg^0 vapour generator,
224 namely a permeation tube, and a gas mass-flow diluting system. The working principles of such a
225 procedure are the dependence on temperature of both dilution of a saturated source of mercury
226 and gas permeation. The final Hg^0 concentration of interest was then obtained by both tuning the
227 temperature of the permeation tube and the dilution flow. Briefly, the homemade PTFE
228 (polytetrafluoroethylene) permeation tube filled with a suitable amount of Hg^0 was coupled to a
229 mass flow controller system (4-Channel-MKS 247) to dilute the mercury-saturated gas with
230 synthetic pure dry air (5.5 grade by Praxair-Rivoira, Italy). Specifically, the permeation tube was
231 introduced into a quartz gas-washing bottle immersed into a thermostat controlled water bath.
232 The permeation rate was first let equilibrating at the temperature of interest (35 °C) under a low
233 flow rate, namely 10 sccm, passing through the mercury reservoir to ensure the gas became
234 saturated with mercury. The mercury-saturated gas was then diluted to the concentration of
235 interest by flowing it into quartz mixing chamber, where it was blended at room temperature
236 together with flowing synthetic dry air. Both gas-washing bottle and mixing chamber were
237 continuously flowed overnight with synthetic dry air to achieve equilibrium, then fixed aliquots of
238 Hg^0 vapour were withdrawn through a PTFE septum using a gas-tight glass syringe, and injected
239 into a measuring chamber consisting of a 100 mL quartz bottle. The Hg^0 concentration in the gas-
240 washing bottle, in the mixing chamber and in the measuring chamber were all checked by
241 Tekran®2537A analyser. Alternatively, Hg^0 vapours were flowed directly into the measuring
242 chamber at selected flow rate values after dilution by air flowed throughout the mixing chamber
243 (Fig.10, *sketch*).

244 A single sensor was housed in each measuring chamber in order to expose the sensitive area to
245 fixed concentrations of elemental mercury vapours. Responses were calculated as $\Delta I/I_0$, where ΔI
246 was the current variation and I_0 was the current when synthetic pure dry air was flowed. A 3 min
247 thermal shot at 450°C under flow of pure air was carried out to restore sensors to the starting
248 current value, after each Hg^0 vapours measurement. The outgoing air from both mixing and
249 measuring chambers were passed through a trap of activated coal to retain the generated Hg^0
250 vapours.

251

252 **3. Results and Discussion**

253

254 *3.1 Morphological investigation of AuNPs/TiO_2 nanofibrous layer*

255 By combining electrospinning and sol-gel techniques, nanofibres made of PVP and amorphous
256 TiO_2 were obtained by injecting the ethanol/acid solution, containing both PVP and TiiP, under a
257 high voltage. The resulting fibres were collected for 20 min on oxidised silicon wafers and IDEs,
258 properly fixed on the surface of a conducting rotating collector to form nonwoven mats. The
259 resulting scaffolds are well known in literature for their high surface areas and relatively small
260 pore sizes **[37]**. One hour electrospinning deposition provided the formation of a thicker white
261 and soft fabric for further possible applications that was easily peeled off [Fig.1,*b*]. This material
262 was hygroscopic and soluble in both water and polar solvents. A 20 min deposition generated a
263 thin fibrous film adhering to substrates. The following calcination resulted in the complete
264 degradation of PVP with formation of crystalline TiO_2. Upon calcination at 550 °C the fibres
265 diameters significantly shrunk. As previously reported by the authors **[37]**, mean diameters of
266 fibres were estimated by SEM images within the range of 60–80 nm with TiO_2 grain size ranging
267 between 5 and 40 nm. The electron diffraction pattern demonstrated that the fibres were
268 composed exclusively of anatase crystalline phase. Calcination of 1 h-fabric made it thinner (upon
269 the diameter shrunk of the fibres), thus resulting in a clearer, glassy and highly brittle material (Fig.
270 1,*c*), but insoluble in water and all organic solvents. The 20 min deposited fibrous layer resulted
271 finely attached to the substrate, as confirmed by electron microscopy images (Figure 1,*d*).

272

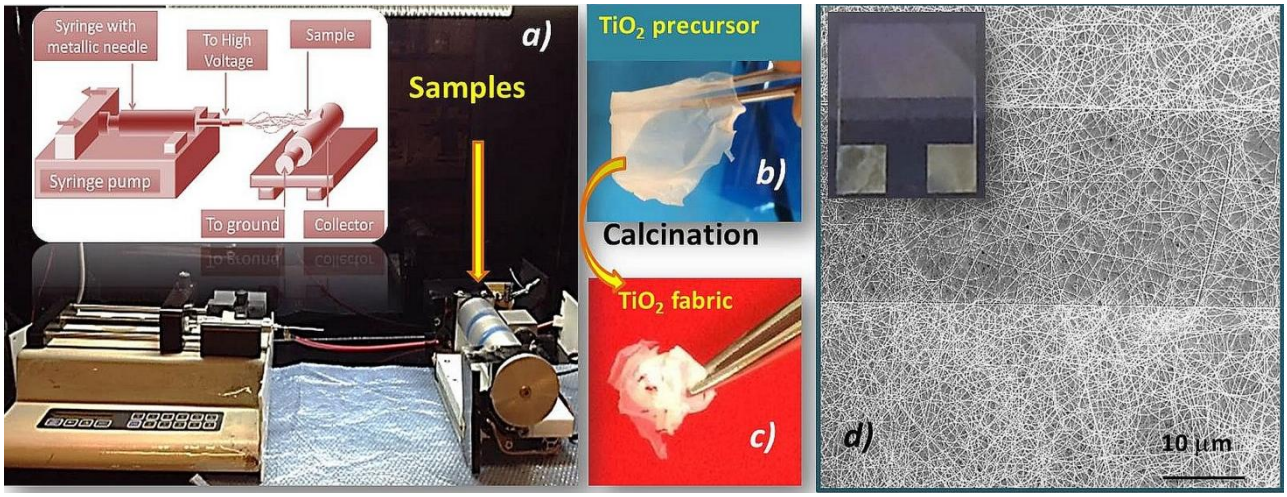

Figure 1. Electrospinning equipment comprising a syringe pump and a grounded rotating cylinder collector where the samples take place for their coverage (*sketch and photograph*) (*a*); a piece of nanofibrous fabric of TiiP/PVP (*b*) after 1 hour of electrospinning deposition and after calcination at 550°C (TiO_2 nanofibrous fabric) (*c*); SEM picture of a dense network of nanofibres of TiO_2 covering IDEs electrodes (*d*). A picture of an IDE coated of nanofibres was reported as inset, too.

273

Titania fibrous layers were decorated with linkers-free gold nanoparticles (AuNPs), by inducing a selective growth upon photocatalytic reduction of $HAuCl_4$ caused by UV light irradiation **[35,40]**. Morphology, size, distribution of gold nanoclusters and the degree of AuNPs coverage of the nanofibres seemed to depend on both UV irradiation exposure, salt concentration and concentrations of organic capping reagent. PVP as an organic polymer and its 0.1 M concentration were chosen according to the scientific literature, because enabling to get regular shaped nanoparticles (i.e. semispheres), when the photocatalytic properties of TiO_2 were used to grow AuNPs on TiO_2 nanofibres **[41]**. In its study, indeed, Wold reported that the absorption of photons by TiO_2 was able to excite electrons from the valence band to the empty conduction band (>3.2 eV), thus generating electron–hole pairs (see the sketch of Fig. 2). The photogenerated holes oxidised water, thus producing hydroxyl radicals capable of oxidising organic compounds (e.g. pollutants) in water, whereas the excited electrons reduced the gold ions on the surface of TiO_2 nanofibres, and induced AuNPs deposition. The photocatalytic process was pointed out by the change in colour of the solution from colourless to deep purple, when a solid substrate covered with anatase nanofibres was dipped into it. A $1.47 \cdot 10^{-3}$ M $HAuCl_4$ solution was firstly prepared and then further dilution were carried out to obtain decreasing salt concentrations, until the minimum concentration providing AuNPs deposition on the fibres was identified.

In the present study, only the fibrous nanocomposites that were electrically active on IDEs will be described. Initially the samples were immersed in the highest concentrated solution and irradiated with UV-light for various times **[40]**: the relationship between the irradiation time and the size and distribution of the gold nanoparticles along the fibres was described. Specifically, a longer exposure generated nanofibres completely covered with Au particles (as confirmed by SEM microanalysis, data not shown) with globular shape merged together and with numerous protruding budding, densely clustered and overlapping. On the contrary, when nanofibres were exposed to UV irradiation for a shorter time (30 min), they appeared more homogeneously coated with round-shaped nanoparticles. Such AuNPs decorated nanostructured scaffolds were investigated and tested as potential sensors for mercury vapours. However, working under the described conditions, a great variability in experiments was observed, probably due to the extremely fast photocatalytic process occurring on titania fibres (starting after a few minutes by UV-irradiation). Then, 60 min was set as UV-light fibre exposure time and the samples were dipped into the diluted solutions. Figure 2 (top images) shows two samples supported on silicon wafers, after irradiation for 60 min and dipping in α and β solutions, left and right, respectively. After UV-

exposure, both solutions turned from clear yellow into orange (α) and red purple (β) colours, respectively, depending on $HAuCl_4$ concentration. In both treatments, the surfaces of the anatase nanofibres observed in SEM micrographs (Fig.2, *left picture*) appeared densely decorated with globular nanoparticles, but size, arrangement and density differed, depending on the salt concentration. AuNPs particles showed a more homogeneous distribution on TiO_2 nanofibres upon dipping in lower $HAuCl_4$ concentrations (α). In these samples, AuNPs mostly appeared individually distributed, i.e. without forming any aggregation structure, when both analysed by SEM (Fig.2, *left picture*) and TEM (Fig. 3,*b*). On the contrary, TiO_2 nanofibres upon dipping in β solution showed aggregation structures of AuNPs with diameter until 90 nm and more (Fig.2, *right picture*, and Fig. 3,*a*). Furthermore, a broader size distribution of AuNPs along nanofibres was observed, when analysed by SEM (Fig.2, *right picture*), TEM (Fig. 3,*a*,*d*). In the CT image the gold nanoparticles appear darker and spherical or quasi-spherical. The single particles size were ranging between 2 and 20 nm and 7.8±3 nm was estimated average diameter (Fig. *3,c*). Approximately spherical structures around 50 nm diameter, densely packed and forming protruding budding along fibres, were sometimes observed along the electrospun TiO_2 nanofibres (Fig. 4,*a,d*)

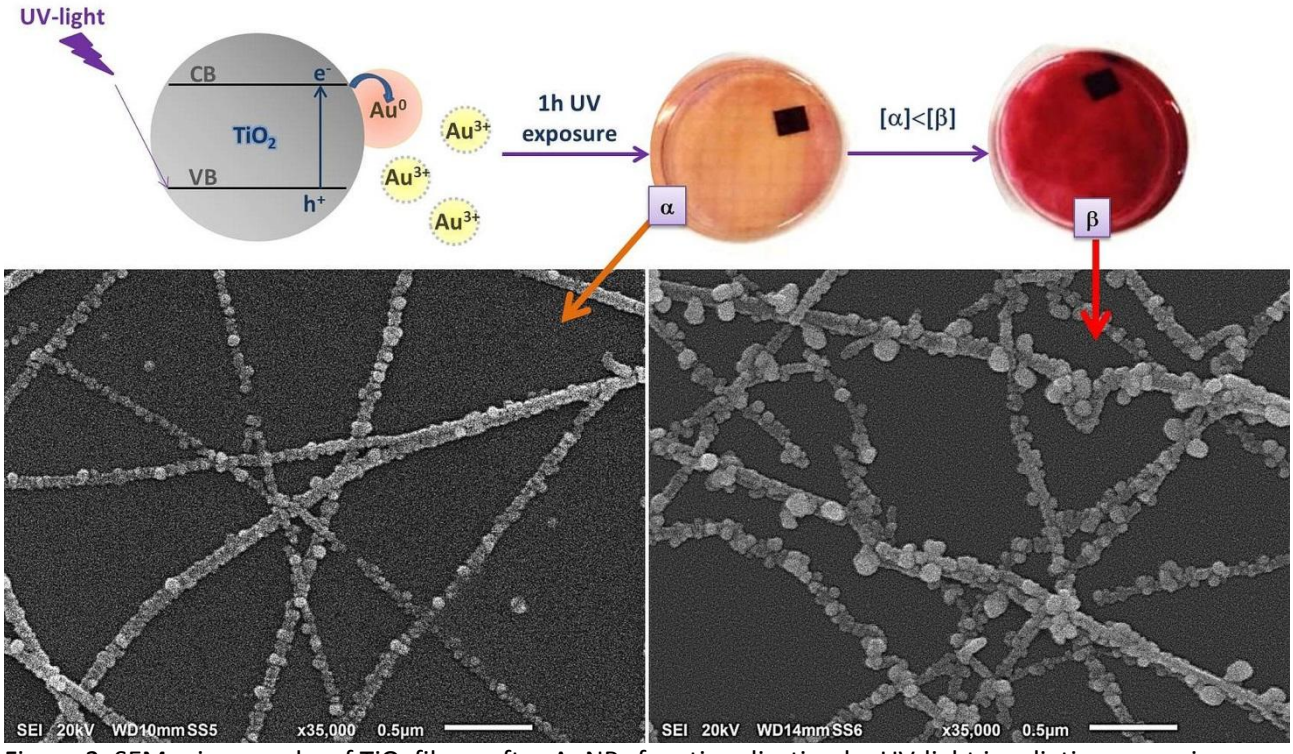

Figure 2. SEM micrographs of TiO_2 fibres after AuNPs functionalization by UV-light irradiation occurring within two $HAuCl_4$ aqueous solutions to lower (*left*) and higher (*right*) concentration, respectively. On the top both a sketch of the photocatalytic process and a picture of the two processed solutions containing the nanofibrous samples were reported.

In Figure 3(*e*), the HRT micrograph shows the contact region between the acicular structure of titania nanofibres and the gold spheres. The interplanar distances measured within the two darker crystals, d= 2.3 Å and d= 2.0 Å , respectively, corresponded to the gold {111} and {200} planes distances, confirming that they were gold.

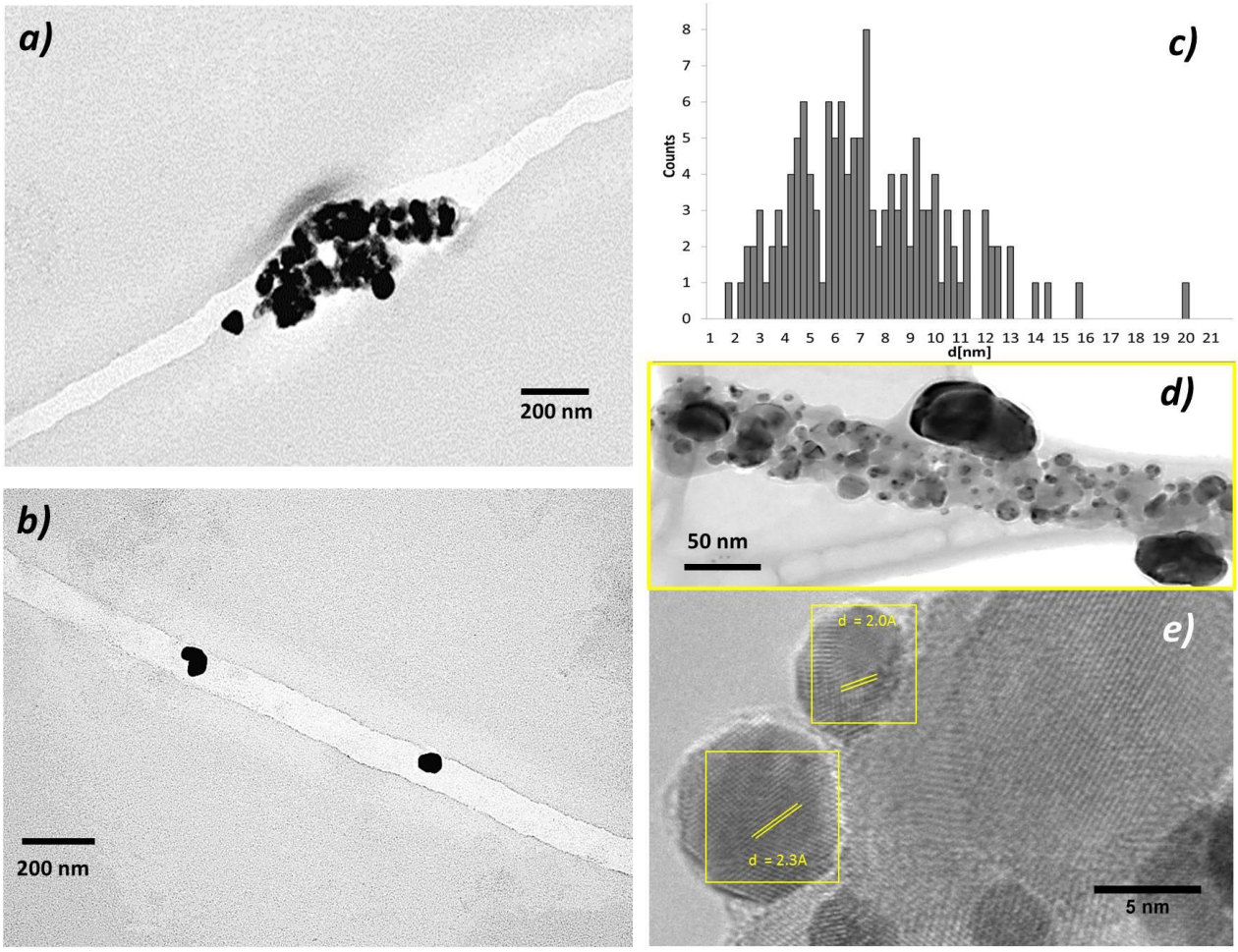

Figure 3. CT micrograph of a titania fibre holding a AuNPs aggregation (β sample) (*a*); CT micrograph of a titania fibre holding a few NPs (α sample) (*b*); bar-graph of the distribution of the diameter values estimated on 150 nanoparticles (*c*); CT image of a gold nanodecorated fibre of TiO_2 (β sample) (*d*); HRT micrograph of contact region between the acicular structure of titania nanofibres and the gold spheres (*e*)

In both chemoresistors and silicon wafers, the TiO_2 nanofibrous layers were still attached to any substrate after the photocatalytic treatment in immersion. Furthermore, gold nanoparticles did not grow directly on the substrates and their immobilisation onto the nanofibres appeared relatively strong (despite due to van der Waals forces), since they both resisted to water rinsing and fibres scratching for TEM analyses. After the photocatalytic treatment, the original calcined white porous scaffold (Fig. 1,*c*) became purple-violet, depending on the size and density of the immobilised AuNPs (data not shown). SEM micrographs reported in Figure 4 confirmed the good

coverage of the electrodes (*a*) and the persistence of the high porosity (*b*) even after AuNPs decoration. AFM micrograph presented in Figure 4 (Fig. 4,*c*) showed a 3D-network of AuNP/TiO_2 nanofibres and their interconnections, which highlighted the absence of any merging effect on nanofibres, both upon UV-irradiation in solution (decoration treatment) and heating (capping agent removal treatment). Furthermore, the presence of long and continuous fibres within the fabric was confirmed.

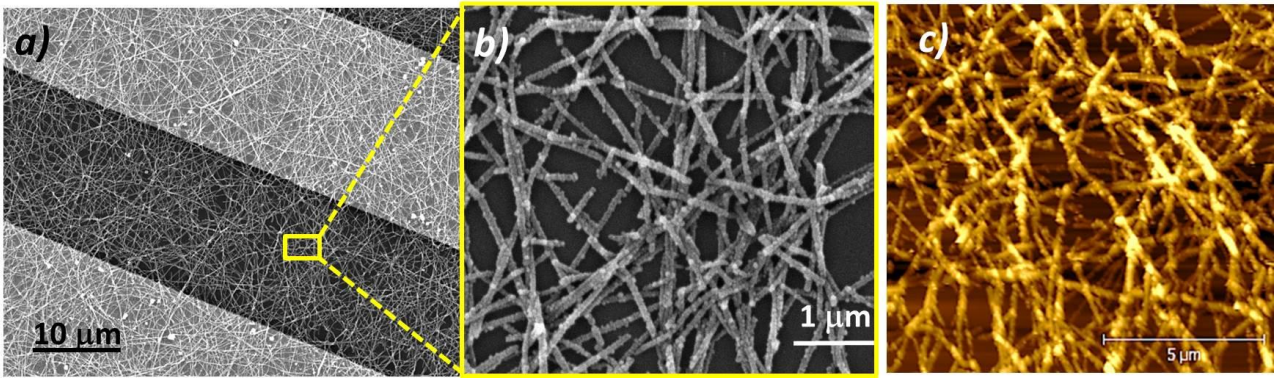

Figure 4. SEM micrographs of TiO_2 fibrous layer coating the electrodes of an IDE after the photocatalytic process (*a*) and magnification of an area (5x5μm) between the two electrodes (*b*); AFM micrograph of the AuNPs/TiO_2 scaffold on silicon wafer (12x12 mm) (*c*)

3.2 Electrical and sensing features

Figure 5 depicts a comparison between Current–Voltage (I-V) curves of Sα and Sβ chemoresistors, treated within [α] and [β] solutions, respectively, when synthetic dry air was flowed. The respective shapes were unaltered when air or nitrogen were flushed over the fibres **[40]**, suggesting that oxygen concentrations poorly affected the electrical properties of chemoresistors. The resistance of IDE coated with undecorated TiO_2 nanofibres resulted to be too high at room temperature to contribute straight to the final current. The resulting linear shape (Ohmic behaviour) within the selected voltage range (−3V to +3V) indicated a constant resistance value for the Sβ (Fig. 5,*b*) and the absence of rectifying contact between the electrodes and developed material. The very low level of resistance (~1.2 kΩ) provided the possibility to work at low voltage, with consequent effects on the lifetime of the material and energy consumption. Moreover, the linearity of I–V curve suggested that the sensing scaffold had a good adherence to the metal electrodes. Vice versa, the Sα showed a non-linear curve (-6V to +6V) (Fig. 5,*a*), probably related to the lower density of the gold-nanoparticles along the nanofibres, suggesting the formation of a Schottky barrier between nanofibrous material and metal electrodes **[42]**.

Regarding Sα and Sβ conductivity at room temperature, it should be due to the metal nanoparticles distributed along the nanofibres and in contact to the electrodes. The electron conductivity could be described by the percolation model **[43]** since the titania at room temperature could be supposed like an insulating organic matrix. In fact, the undoped anatase is an anisotropic, tetragonal insulator (with a bandgap of 3.2 eV). When it is metal doped, the electron conductivity is dominated by thermally activated electron tunneling from one metal island to the other. However, the conductivity of the nanocomposite is lower than that of pure metal (gold) because the electron mean free path is greatly reduced due to the inclusion of the dielectric (the titania crystals). Above the percolation threshold, continuous metallic pathways exist throughout the metal oxide matrix. In the percolation zone, adjacent metallic nanoparticles undergo extensive coalescence resulting in large irregular nanoclusters. The increase in electrical conductivity results from an increased connectivity of the metallic nanostructures, depending on the fibres size and the metal loading. The AuNPs within the Sβ , although irregular in size, were spaced from each other just a few nm (about 2 nm), whereas longer distances among NPs were estimated in Sα. Photonic and thermal energy commonly enable these devices to overcome the energy gap. In the present study, only the chemoresistors showing Ohmic behaviour in air and at room temperature (Sβ) were investigated for convenience in mercury vapour detection.

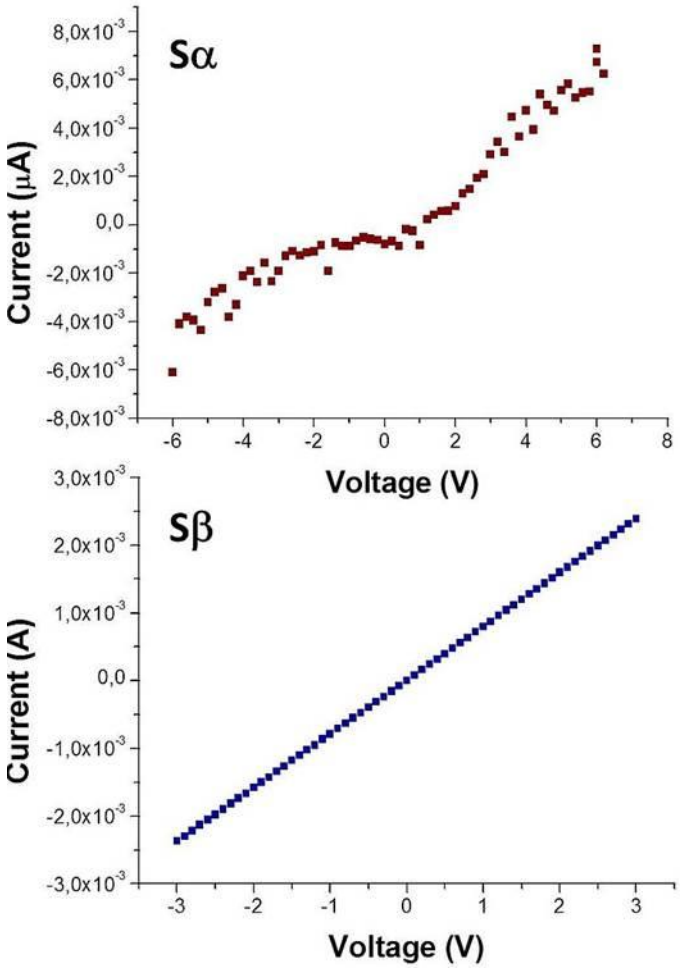

Figure 5. Current-Voltage curves of Sα (*up*) and Sβ (*down*) chemoresistors

375

376 Several sensors (Sβ) were fabricated in laboratory in order to check their reproducibility. Within a
377 set of 20 chemoresistors fabricated in distinct periods over five months the mean resistance value
378 was estimated to be about 1349,95 Ω, S.D.=±150,25 with a minimum of 1020 Ω and a maximum
379 of 1600 Ω (Fig.6).

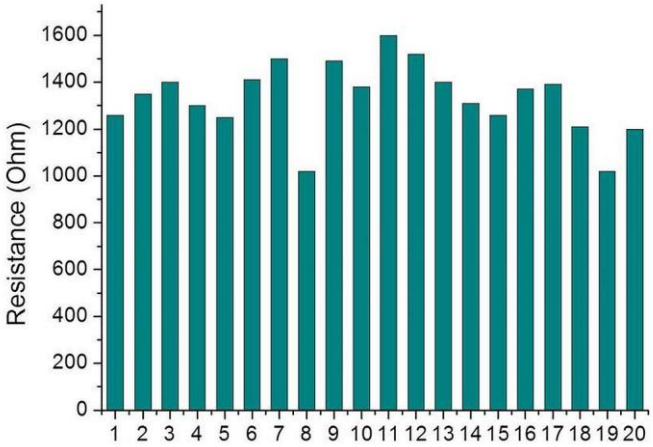

Figure 6. Bar-graph depicting the resistance values of 20 chemoresistors (Sβ types)

The sensor measurements, that were the electrical signals reported when interaction between the sensing layers and the analytes were occurring, resulted in a change of the whole resistance (or current, i.e. I =V/R according to Ohm's law) of the device according to the following Eq:

$$R = \frac{1}{2N-1}\rho\frac{\omega}{h \cdot L}$$

where N and L are number and size of the fingers, h and ω the electrode thickness and width, respectively, and ρ resistivity of the overlying material. Such a planar interdigitated electrode configuration is the most commonly used for conductometric sensing applications. A picture of an electrode is reported in Figure 1,*d*. At one end of the structure there is a set of interdigitated electrodes which occupies an area approximately 3x5 mm; at the opposite end of the chip there are two bonding pads (2x2 mm) connected to the electrometer (DC voltage). Sensing measurements, i.e. current (or resistance) changes, were provided both in continuous and with pulse of potentials applied every a few minutes. The second strategy was tested in order to investigate the possibility to further decrease the power consumption, allowing the sensor to work by battery for quite a long time. Furthermore, in order to investigate the contribution of the measuring system to the sensor features, mercury was detected by injecting a defined volume of polluted air and by flushing known concentration of mercury throughout the measuring chamber.

When a volume of air polluted with a known concentration of Hg^0 was injected or flowed into the measuring chamber, Sβ exposed to mercury vapours showed a decrease in current. In detail, when about 74 ppt Hg^0 were injected in the measuring chamber, the measured current value decreased with a rate of $\sim$ -1.93·10^{-5} min^{-1} ($(I/I_0)/t$) until reaching a signal decrement of -3.7·10^{-3} ($\Delta I/I_0$) after ~200 min. In Figure 7 the sensor current values after injection, normalized to the starting current in dry air free from mercury, have been reported when pulses of potential (+1V) were applied. The limit of detection, calculated as three times the standard deviation of the blank, was about 6 ppt. Despite the high sensitivity of the chemosensors to Hg^0 vapour, the response appeared to be slow, when injection procedure was used, probably due to the diffusion rate of mercury (0.14 cm^2s^{-1}**[44]**) into the measuring chamber (100 ml) and then the following adsorption onto the nanoparticles within the titania fabric. One potential solution for decreasing the response time could be achieved by designing a geometry of injection with a flow impacting perpendicularly the sensing area facilitating the adsorption of mercury onto the gold-nanoparticles. Indeed the

flow rate impacts the transfer of Hg to the AuNPs surface (mass transfer) and thus reduces the sensor's response time **[32]**. However in this study only the surface adsorption, unrelated to mass transfer, was investigated and the flow throughout the measuring chamber didn't impact to the sensor surface. The response time taken to achieve 90% of the equilibrium point was ~180 min. Similarly the Hg^0 vapours were flowed directly throughout the measuring chamber and a remarkable improvement in response time was achieved, as expected (an increase of the mass flow rate of mercury per time unit). In Figure 8 is depicted the comparison between the curve slopes of the normalised sensor responses to the same concentration of Hg^0, when injected and flowed (the black and red lines, respectively). A comparison between the normalised sensor responses per concentration unit versus time reported an increase of an order of magnitude when the same concentration of the analyte was injected ($2.62 \cdot 10^{-7}$ ppt^{-1}) and flowed ($2.16 \cdot 10^{-6}$ ppt^{-1}), respectively (Fig. 8). However, since previously the authors reported that nanostructured material could adsorb Hg^0 vapour up to change the chemosensor resistance value by 30% **[40]**, a continuous flow of the analyte over the material was able to cause a continuous decrease in current over a long time. This effect is presumably due to the kind of interaction between mercury and gold. Indeed, the adsorption constant is orders of magnitude higher than the desorption constant, justifying the limited desorption at near room temperatures **[32]**. Mercury adsorption proceeds towards a sub-monolayer until the available sites are full (Langmuir isotherm model). After surface adsorption, additionally, the formation of islands of amalgam occurs hindering the release of mercury in the environment. Indeed, mercury desorption can occur by changing the vapour partial pressure only at the initial phase of the interaction. The fabricated nanostructured chemosensors could be compared to a 3D-conductive trap for mercury vapour, which works until the saturation of all the interacting sites occurs. A complete desorption of mercury occurred heating the sensing area covered by the fibres up to 450 ° C for 3 min, after each measurement. In fact, current resulted completely recovered after this treatment, as reported in Fig. 9,*b*. The sensor was exposed to a flow of mercury in dry air with a concentration of 800 ppb for 5 min (Fig. 9,*a*), and then dry air was used to clean the sensor surface. The current curve trend slightly changed when clean air was flowed, stabilizing at about the current values reached for Hg^0 adsorption. Due to the strong affinity between gold and mercury, only thermal treatments were able to remove mercury. Sensor was heated at 550°C for 10 s and 30 s, respectively, and the current was measured under pure air showing only a partial restoring of the starting current, thus suggesting that a treatment of 3 minutes was necessary to get the same starting current value. Thereafter,

the sensor was placed in a suitable gas-washing tube of quartz (75 ml) and heated at 550°C for 5 min in oven under dry air flow (1L/min). The air flushing the sample was delivered to the mercury analyser: no more Hg was detected in the sensor headspace, confirming that the analyte was completely removed by the fibrous layer.

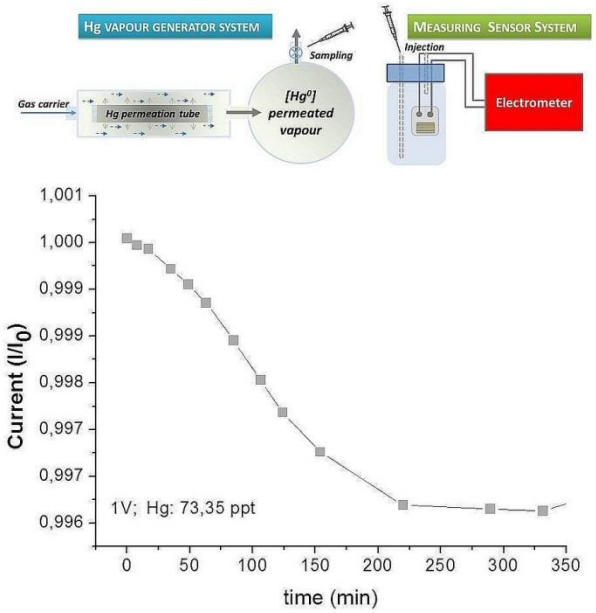

Figure 7. Normalised transient response of Sβ chemosensor when Hg^0 ~74ppt was injected into the measuring chamber. Pulses of potential were applied every a few minutes (V=+1V) and current values were recorded (y-axes) over time (x-axes). On the top a drawing of the measuring system set-up.

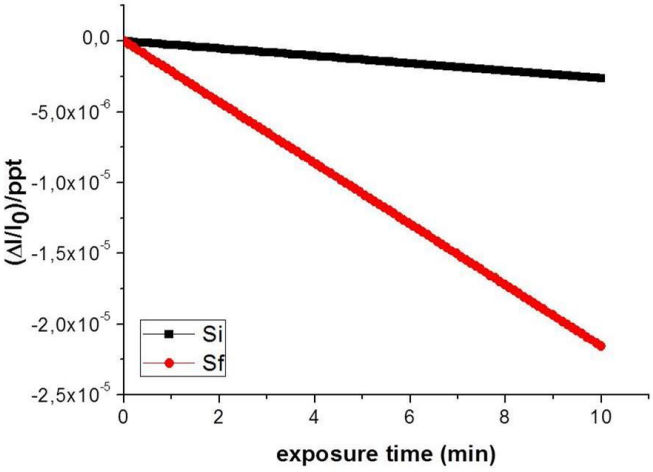

Figure 8. Comparison of the sensor normalised response rates per ppt over 10 min when Hg^0 was injected (Si) or flowed (Sf) into the measuring chamber

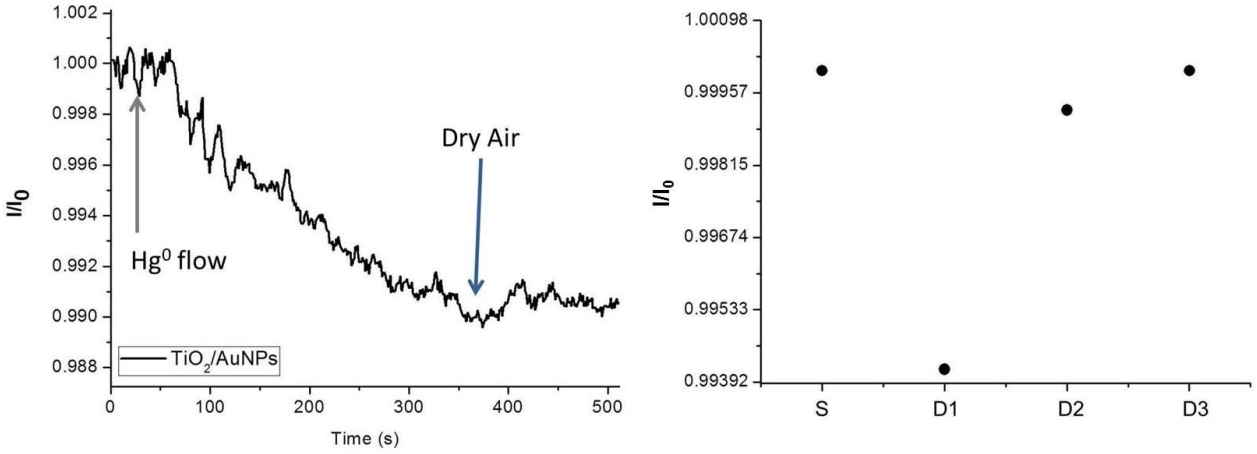

Figure 9. Transient sensor response when Hg^0 800 ppb was flowed throughout the measuring chamber for about 5 min, followed by dry air flushing (*a*); normalized current values before mercury exposure (S), after mercury exposure and 450°C heating treatments for 10 s (D1), 30 s (D2) and 3 min (D3), respectively (*b*)

In order to test the responsiveness of the device to Hg concentration lower than 74 ppt Hg^0, mercury vapours were flushed throughout the measuring chamber. The final Hg^0 concentration was obtained by tuning the dilution flow (Fig.10,*sketch*). Preliminary results showed that the sensor exposure to 45 ppt of Hg^0 resulted in a decrease in current, with a rate of ~$-9.7 \cdot 10^{-5}$ min^{-1} (i.e. 5 times faster than by injection). After 60 min of measurement, the normalised current was 0.7% decreased, and the limit of detection was estimated about 1.97 ppt. When the concentration of Hg increased, the response curve slope changed too. Specifically, when the sensor was exposed to 800 ppb, the current decreased more quickly with a rate of ~$-9 \cdot 10^{-3}$ s^{-1} (Fig.9,*a*). On the other hand, a continuous mercury flowing involved a likewise continuous adsorption of the analyte to the gold free sites, thus hindering the sensor to reach the steady state unless the all binding sites saturation. A decrease in resistance value of the sensor up to 30% was reported **[40]** when sensor was exposed to a mercury saturated vapour pressure (P_{V0}) for 12 h.

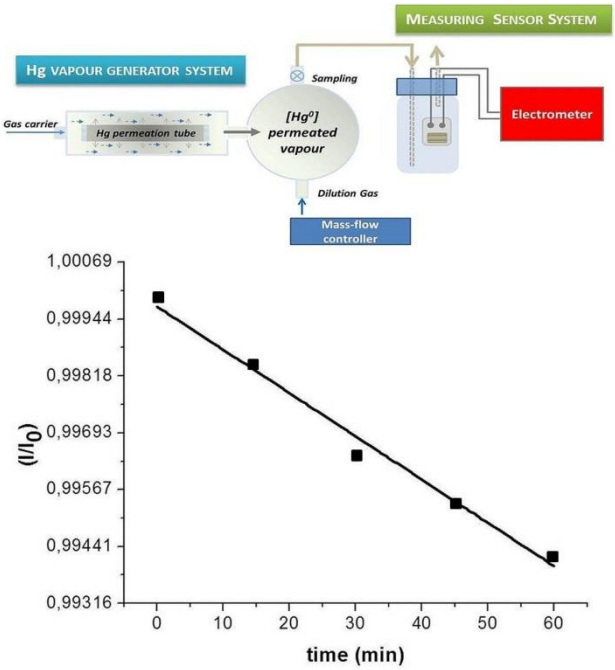

Figure 10. Normalised current decrease of Sβ when Hg^0 45 ppt was flowed throughout the measuring chamber for 1 hour. On the top a drawing of the measuring system set-up

Since at room temperature and in dark condition the measured current is supposed to be due to AuNPs decorating titania fibres, only chemical compounds interacting with gold are expected to be mostly responsible of the current changes: halide and sulphide are the main eligible interfering compounds. Thus in a cocktail of other chemicals, this sensor has been designed as a pretty selective sensor, being able to greatly decrease the environmental disturbances allowing the investigator/manufacturer to design and then fabricate easier strategies to prevent contaminations from environment (selective filtering systems or coatings). Among common potential contaminants authors investigated previously water vapour influence (%RH) reporting no-effects on the electrical signals **[40]**.

Conclusions

The ability of Hg to be re-distributed in the environment through a complex combination of physical, chemical and biological processes, has received increasing attention in recent years and has enhanced the need for a global action in ruling and monitoring its releasing in the atmosphere. It is largely recognised that Hg contamination of the ecosystems and the consequent human exposure remains a serious hazard. Since the need for fast detection systems to be used for large area monitoring, at low cost and low maintenance, as well as ease of use are becoming ever more urgent, sensors and sensing systems looked the most promising alternative to the traditional

instruments. The mainly sensing strategy has focused on the strong affinity of mercury to gold, and more recently thanks to the advances in nanotechnology, to nanostructured gold materials (such nanoparticle, nanowires and nanorods). Exploiting the photocatalytic properties of electrospun titania fibres, a conductometric sensor has been designed and fabricated to detect elemental mercury in air. Thus, gold nanoparticles have been grown on nanofibrous scaffolds of TiO_2 by photocatalysis. Electrospinning technology has been used successfully to create a 3D-framework of titania covering the electrode sensing area of the properly designed chemoresistors (IDEs). Its electrical properties, depending on shape, size and number of gold nanoparticles decorating the fibres, were easily tuned, showing the sensor was able to work at room temperature and highly sensitive to Hg^0 (tens of ppt). The sensor is expected to be robust since it is composed with titania and gold, two chemical compounds considered among the most robust materials since resistant to common solvents and VOCs as well as microorganisms attacks. Additionally, the sensor has been designed to work at room temperature being thermally treated (450°C) only for a few minutes up to desorb mercury from AuNPs, thus thermal drift effects are expected to be lowered. An encouraging reproducibility in laboratory fabrication of the chemoresistors was obtained (R_m=~1.3 kΩ). The fabricated nanostructured chemosensors worked as Hg^0 vapours highly adsorbing 3D-conductive traps, capable of working until the saturation of all the interacting sites occurred. Depending on the strategy of sampling, the limit of detection could be improved, ~6 ppt when mercury vapour was injected and ~2 ppt when slowly flowed within the measuring chamber. However, despite the high sensitivity of the chemosensors to Hg^0 vapour, the responses appeared to be slow. Further investigations are necessary also to assess the effects of physical parameters of the environment, such as temperature fluctuations and UV-light, as well as chemical ones, such as volatile organic compounds and gas (like halides and sulphides) which are potentially interfering the adsorption process of the Hg^0 on gold. The ease of deposition (electrospinning) and preparation (UV-irradiation in aqueous solution) as well as the high Hg^0 sensitivity, suggests the chance to investigate the material features by further transduction systems.

Acknowledgments

The activity is part of the International UNEP-Mercury Programme (UNEP-Mercury Air Transport and Fate Research (UNEP-MFTP) within the framework Global Mercury Observation System, funded by EC as part of EC FP7.

References

1] EG. Pacyna, JM. Pacyna, K. Sundseth, J. Munthe, K. Kindbom, S. Wilson, F. Steenhuisen, P. Maxson. Global emission of mercury to the atmosphere from anthropogenic sources in 2005 and projections to 2020. Atmospheric Environment 44 (2010) 2487–2499

2] N. Pirrone, R. Mason. Mercury Fate and Transport in the Global Atmosphere (Emissions, Measurements and Models), pp. 1-637, Springer US 2009. DOI.10.1007/978-0-387-93958-2

3] DW. Boening. Ecological effects, transport, and fate of mercury: a general review, Chemosphere 40 (2000) 1335±1351

4] HE. Ratcliffe, E. Hope, GM. Swanson,LJ. Fischer. Human exposure to mercury: a critical assessment of the evidence of adverse health effects. Journal of Toxicology and Environmental Health 49 (1996) 221-279

5] TW. Clarkson. The Toxicology of Mercury. Critical Reviews in Clinical Laboratory Sciences 34 (1997) 34 369-403

6] M. Harada. Minamata Disease: Methylmercury Poisoning in Japan Caused by Environmental Pollution. Crit. Rev. Toxicol.25 (1995) 1–24

7] F. Bakir, S. F. Damluji, L. Amin-Zaki, M. Murtadha, A. Khalidi, N. Y. Al-Rawi, S. Tikriti, H. I. Dhahir, T.W. Clarkson, J. C. Smith, and R. A. Doherty. Methylmercury Poisoning in Iraq. Science 181 (1973) 230–241

8] http://www.gmos.eu

9] http://www.mercuryconvention.org/

10] D. Jaffe, S. Strode. Sources, fate and transport of atmospheric mercury from Asia. Environ. Chem. 5 (2) 2008 121–126

11] M. Ghaedi, MR. Fathi, A. Shokrollahi, F. Shajarat. Highly Selective and Sensitive Preconcentration of Mercury Ion and Determination by Cold Vapor Atomic Absorption Spectroscopy. Analytical Letters 39 (2006) 1171-1185

12] D. Sánchez-Rodas, WT. Corns, B. Chen, PB. Stockwell. Atomic Fluorescence Spectrometry: a suitable detection technique in speciation studies for arsenic, selenium, antimony and mercury. J. Anal. At. Spectrom. 25 (2010) 933-946

13] N. Ferrua, S. Cerutti, J. A. Salonia, R. A. Olsina, and L. D. Martinez. On-line preconcentration and determination of mercury in biological and environmental samples by cold vapor-atomic absorption spectrometry. J. Hazard. Mater. 141 (2007) 693–699

14] Global Mercury Assessment 2013: Sources, emissions, releases, and environmental transport 2013 pp. 1-42, UNEP, ISBN: DTI/1636/GE; http://www2.epa.gov/international-cooperation/mercury-emissions-global-context

15]Battistoni, C.; Bemporad, E.; Galdikas, E.; Kaciulis, S.; Mattogno, G.; Mickevicius, S.; Olevano, V. Interaction of mercury vapour with thin films of gold. Appl. Surf. Sci. 1996, 103, 107–111

16] J Drelich, C. L. White, and Z. Xu. Laboratory Tests on Mercury Emission Monitoring with Resonating Gold-coated Silicon Cantilevers. Environ. Sci. Technol. 42 (2008) 2072–2078

17] K Jasek, S. Neffe, M. Pasternak. SAW Sensor for Mercury Vapour Detection. Acta Physica Polonica A, 122 (2012) 825-828

18] K. Kabir, Y Sabri, G Matthews, L Jones, S Ippolito, S Bhargava. Selective detection of elemental mercury vapor using a surface acoustic wave (SAW) sensor. Analyst (in press) DOI. 10.1039/C5AN00360A

19] YM Sabri, S.J. Ippolito, J. Tardio, A.J. Atanacio, D.K. Sood, S.K. Bhargava. Mercury diffusion in gold and silver thin film electrodes on quartz crystal microbalance sensors. Sensors and Actuators B 137 (2009) 246–252

20] E.P. Scheide, J.K. Taylor, Piezoelectric sensor for mercury in air, Environmental Science & Technology, 8 (1974) 1097–1099

21] K. M. Mohibul Kabir, SJ Ippolito, GI. Matthews, SB Abd Hamid, YM Sabri, SK. Bhargava, Determining the Optimum Exposure and Recovery Periods for Efficient Operation of a QCM Based Elemental Mercury Vapor, Sensor Journal of Sensors 2015, 727432-9

22] J. Mcnerney, R. Hanson, and P. Buseck. Mercury Detection by Means of Thin Gold Films. Science 178 (1972) 611-612

23] V. Raffa; B. Mazzolai; V. Mattoli; A. Mondini; P. Dario. Model validation of a mercury sensor, based on the resistivity variation of a thin gold film. Sensors And Actuators. B, Chemical 114 (2006) 513-521

24] W Chemnasiri, FE. Hernandez, Gold nanorod-based mercury sensor using functionalized glass substrates. Sensors and Actuators B 173 (2012) 322–328

25] JZ. James, D. Lucas, CP. Koshland. Elemental mercury vapor interaction with individual gold nanorods. Analyst 2013 (138) 2323-2328

26] JZ. James, D. Lucas, CP. Koshland. Gold Nanoparticle Films As Sensitive and Reusable Elemental Mercury Sensors. Environ. Sci. Technol. 46 (2012) 9557−9562

27] A. Merkoci. Electrochemical biosensing with nanoparticles FEBS Journal 274 (2007) 310–316

28] N. Ratner, D. Mandler Electrochemical Detection of Low Concentrations of Mercury in Water Using Gold Nanoparticles**,** Anal. Chem., 2015, 87 (10), pp 5148–5155

29] Z-M Dong, X-M Qing, G-C Zhao, Highly Sensitive EQCM Sensor for Mercury Determination by Coupled Stripping Voltammetry Int. J. Electrochem. Sci., 10 (2015) 2602 – 2612

30] YM Sabri, SJ Ippolito, AP O'Mullane, J Tardio, V Bansal, SK Bhargava. Creating gold nanoprisms directly on quartz crystal microbalance electrodes for mercury vapor sensing. Nanotechnology 22 (30) (2011) 305501. DOI 10.1088/0957-4484/22/30/305501

31] S. Keebaugh, WJ Nam, SJ Fonash, Manufacturable Higly Responsive Gold Nanowire Mercury Sensors, NSTI-Nanotech 3 (2007) 33-36, www.nsti.org. ISBN. 1420061844

32] J Crosby. Mercury Detection with Gold Nanoparticles. Electronic Thesis and Dissertations UC Berkeley (2013) http://eprints.cdlib.org/uc/item/3s40h5m0

33] TP McNicholas, K Zhao, C Yang, SC. Hernandez, A Mulchandani, NV. Myung and MA. Deshusses, Sensitive Detection of Elemental Mercury Vapor by Gold-Nanoparticle-Decorated Carbon Nanotube Sensors, J. Phys. Chem. C 2011, 115, 13927–13931

34] A. Macagnano, E. Zampetti, E. Kny, Electrospinning for High Performance Sensors, Springer International Publishing, pp. 1-329, 2015. DOI. 10.1007/978-3-319-14406-1

35] D Li, JT. McCann, M Gratt, Y Xia. Photocatalytic deposition of gold nanoparticles on electrospun nanofibers of titania, Chemical Physics Letters 394 (2004) 387–391

36] Y Yuan, Y Zhao, H Li, Y Li, X Gao, C Zheng, J Zhang. Electrospun metal oxide–TiO2 nanofibers for elemental mercury removal from flue gas, Journal of Hazardous Materials, 227–228 (2012) 427–435

37] E. Zampetti, S. Pantalei, A. Muzyczuk, A. Bearzotti, F. De Cesare, C. Spinella, A. Macagnano. A high sensitive NO_2 gas sensor based on PEDOT-PSS/TiO_2 nanofibres, Sensors and Actuators B 176 (2013) 390-398

38] D. Li, Y. Xia, Fabrication of titania nanofibres by electrospinning, Nano Letters 3 (2003) 555–560

39] J. Ayache, L. Beaunier, J. Boumendil, G. Ehret, D. Laub. In Sample Preparation Handbook for Transmission Electron Microscopy; Anderson, R., Ed.; Springer: New York, 2010; Chapter 4, pp 153−228

40] A. Macagnano, E. Zampetti, V. Perri, A. Bearzotti, F. Sprovieri, N. Pirrone, G. Esposito, F. De Cesare, Photocatalytically Decorated Au-nanoclusters TiO2 Nanofibres for Elemental Mercury Vapor Detection, Procedia Engineering 120 (2015) 422–426

41] A. Wold. Photocatalytic properties of titanium dioxide (TiO2). Chem. Mater. 5 (1993) 280-283

42] BL. Sharma. Metal-Semiconductor Schottky Barrier Junctions and Their Applications. 1984 Plenum Press –New York DOI. 10.1007/978-1-4684-4655-5

43] KH Müller, G. Wei, B. Raguse, J. Myers. Three-dimensional percolation effect on electrical conductivity in films of metal nanoparticles linked by organic molecules. Phys. Rev. B 68, 155407

44] G. A. Lugg. Diffusion coefficients of some organic and other vapors in air. Anal. Chem., vol. 40,no. 7, pp. 1072–1077, 1968.

45] N. Pirrone, W. Aas., S. Cinnirella, R. Ebinghaus, I. M. Hedgecock, J. M. Pacyna, F. Sprovieri, E. M. Sunderland (2013) Toward the next generation of air quality monitoring: Mercury. Atmospheric Environment, doi:10.1016/j. atmosenv.2013.06.053.

46] Lubick, N., Funding Struggle for Mercury monitoring (2013) Nature, 459, 620-621 (2009) | doi:10.1038/459620b

47] S. Cinnirella, F. D'Amore, M. Bencardino, F. Sprovieri, N. Pirrone, The GMOS cyber(e)-infrastructure: advanced services for supporting science and policy, Environmental Science and Pollution Research 21 (2013) 4193-4208

641 **48]** http://www.unep.org

Figure(1)

Click here to download high resolution image

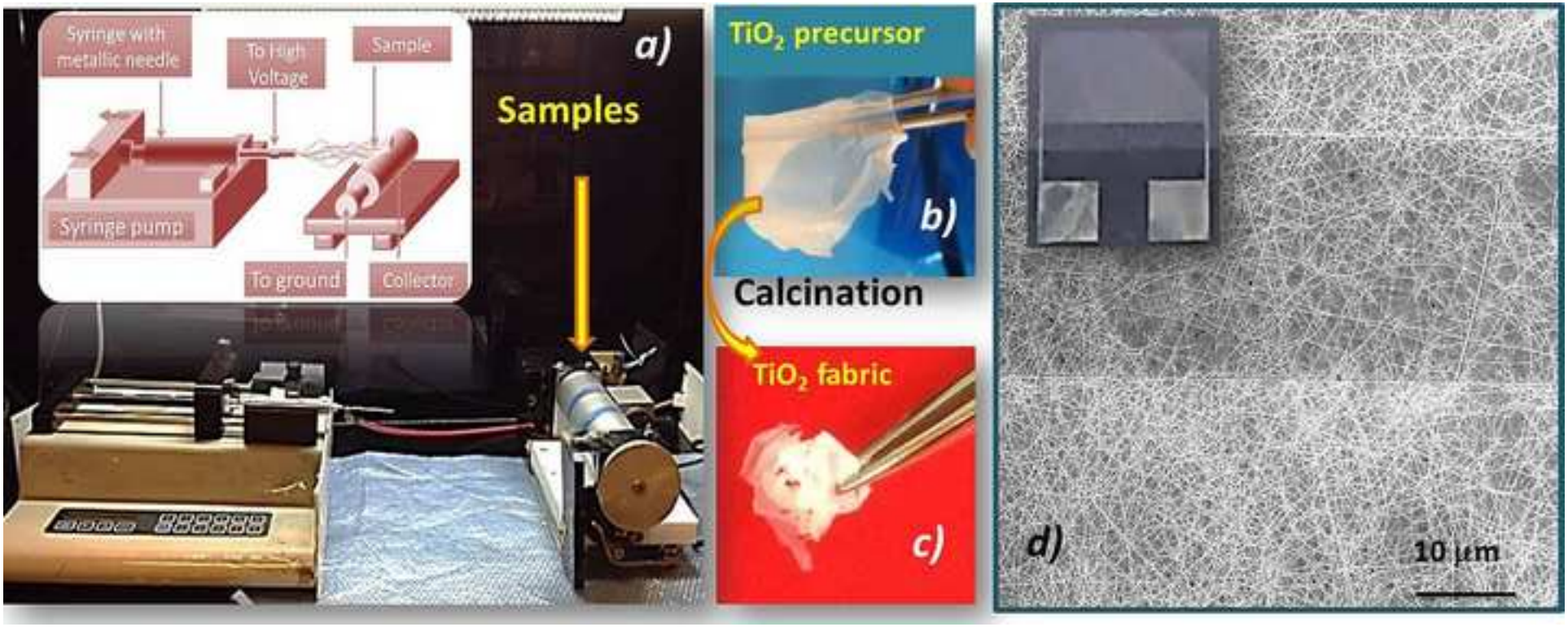

Figure(2)
Click here to download high resolution image

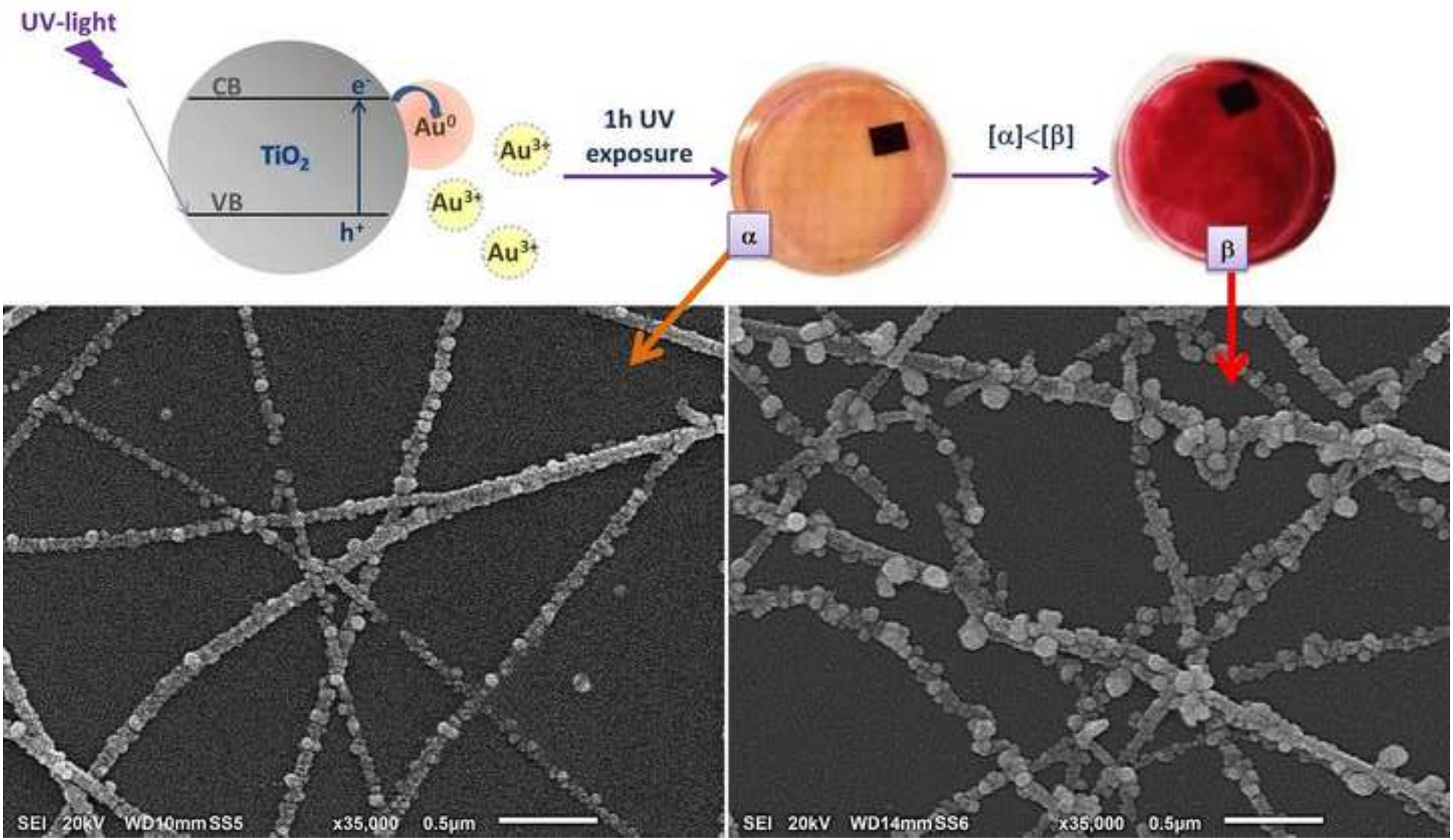

Figure(3)
Click here to download high resolution image

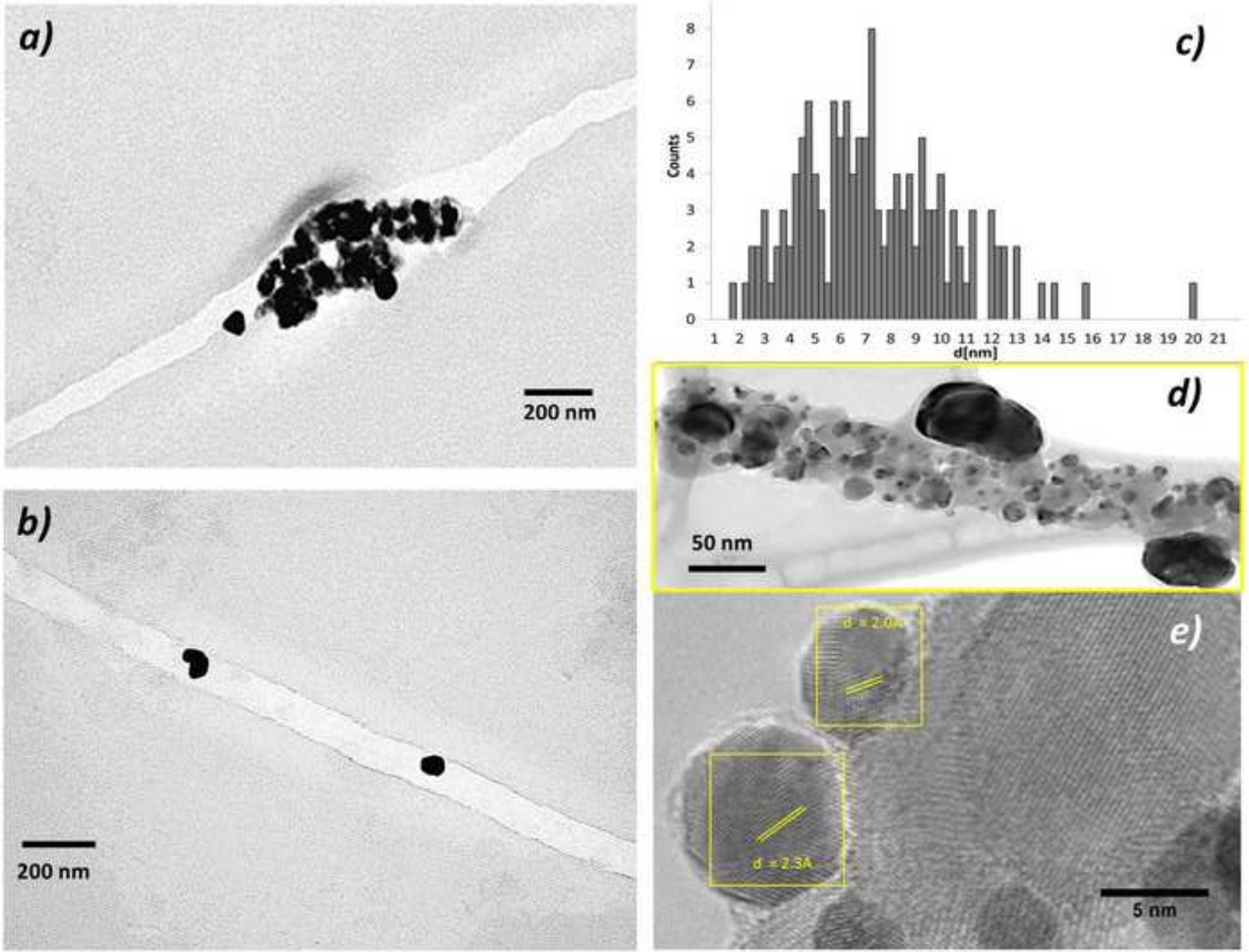

Figure(4)
Click here to download high resolution image

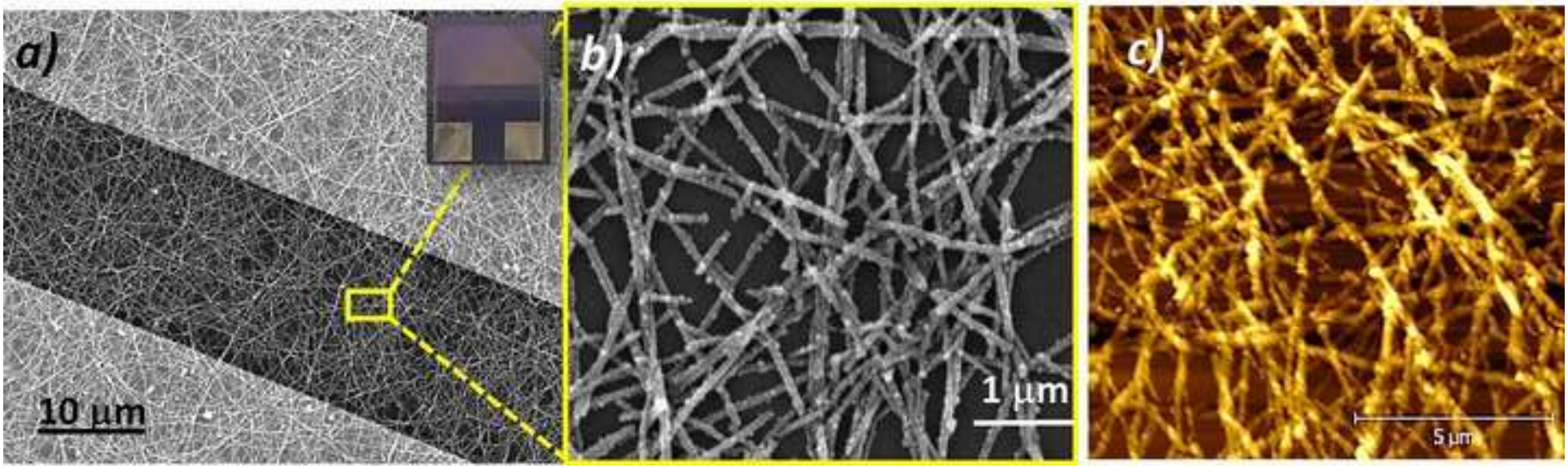

Figure(5)
Click here to download high resolution image

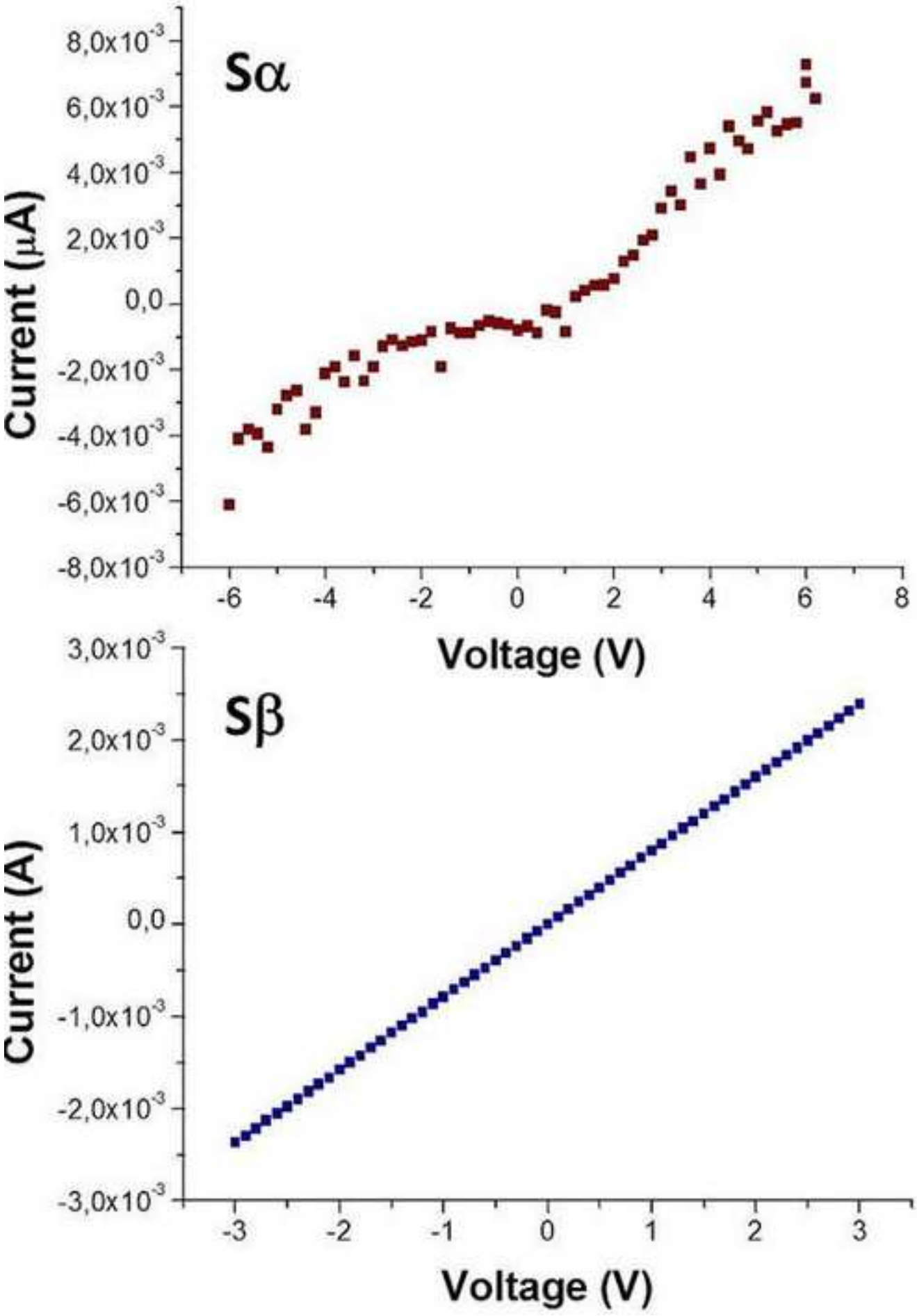

Figure(6)
Click here to download high resolution image

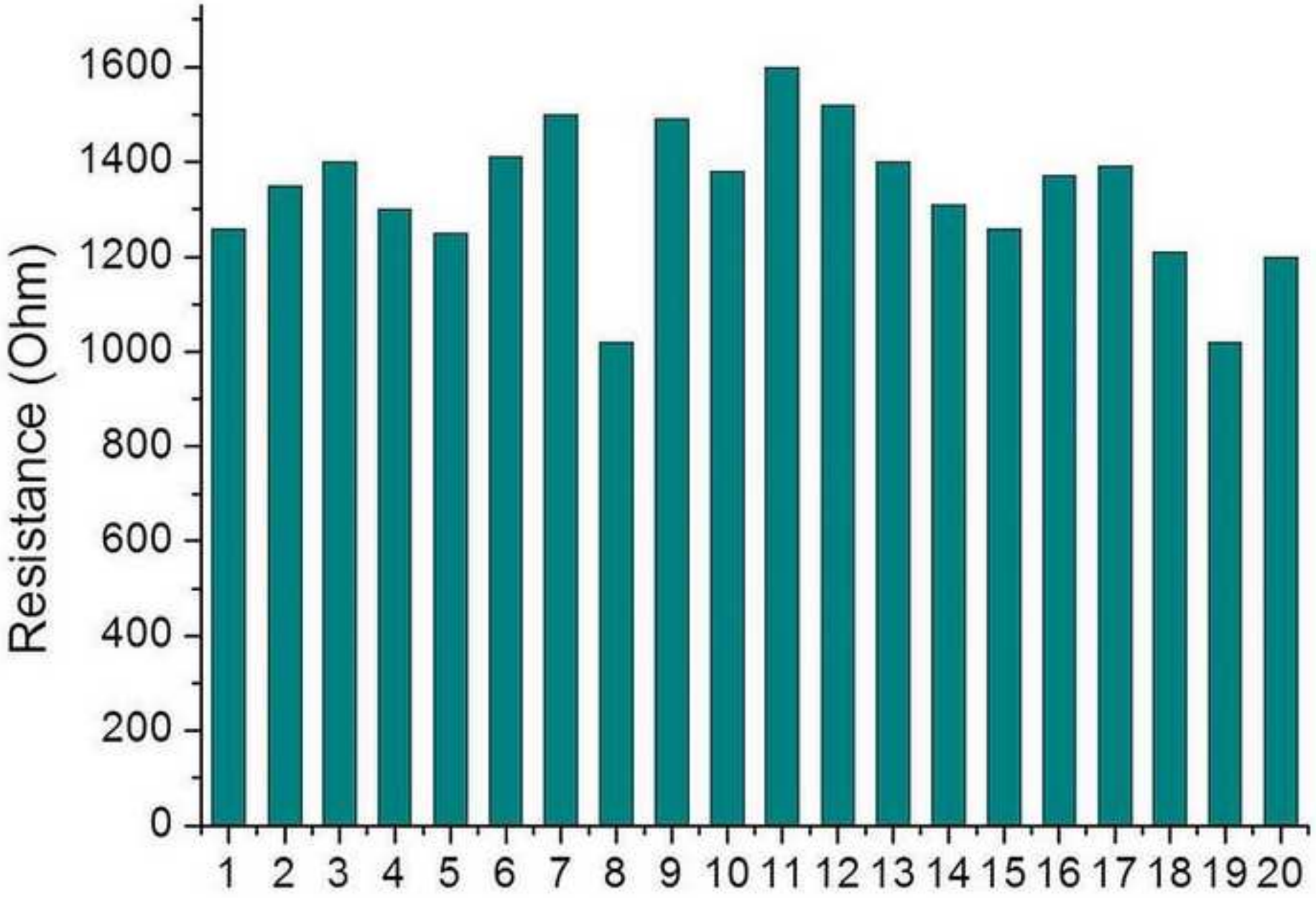

Figure(7)
Click here to download high resolution image

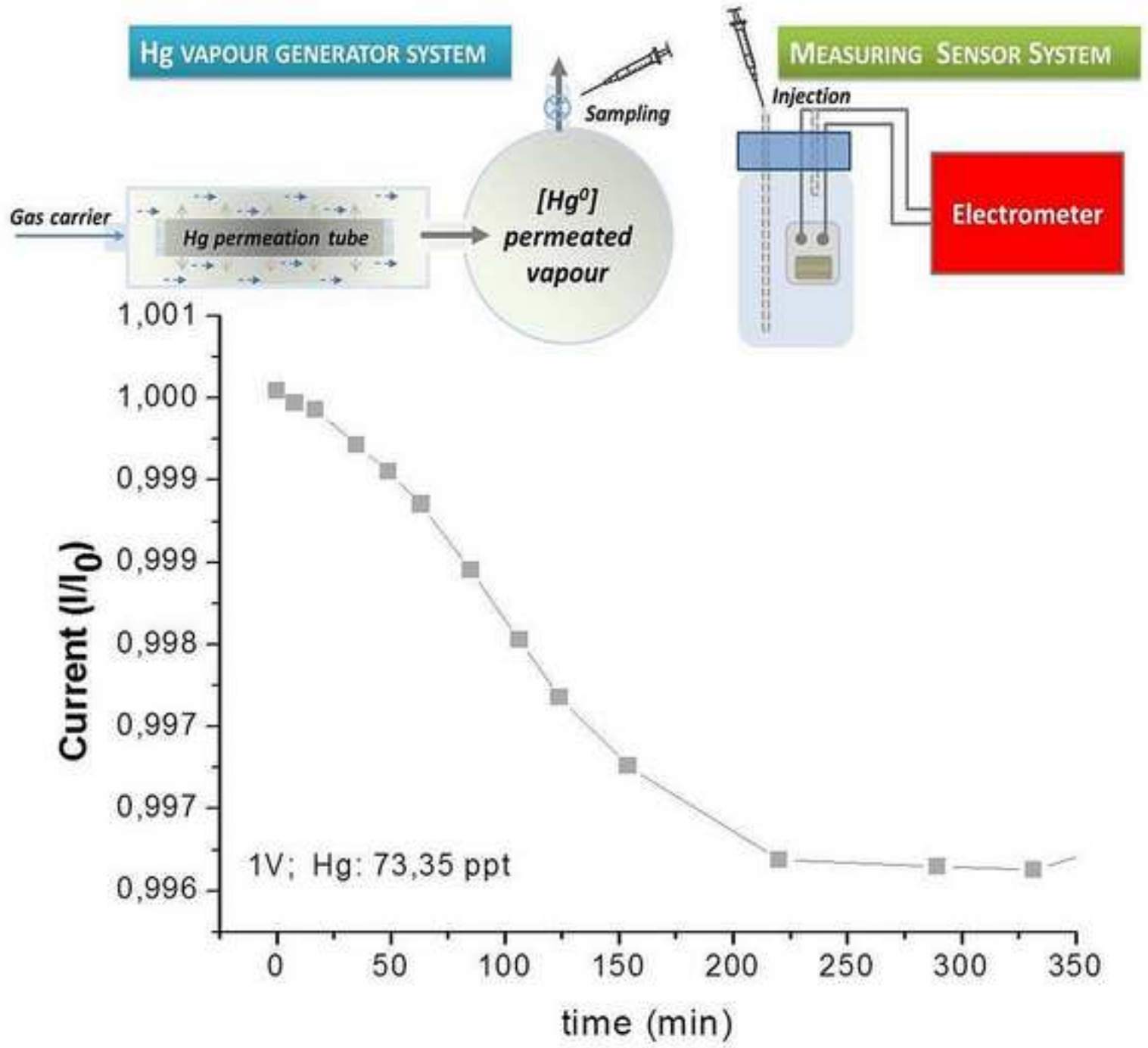

Figure(8)
Click here to download high resolution image

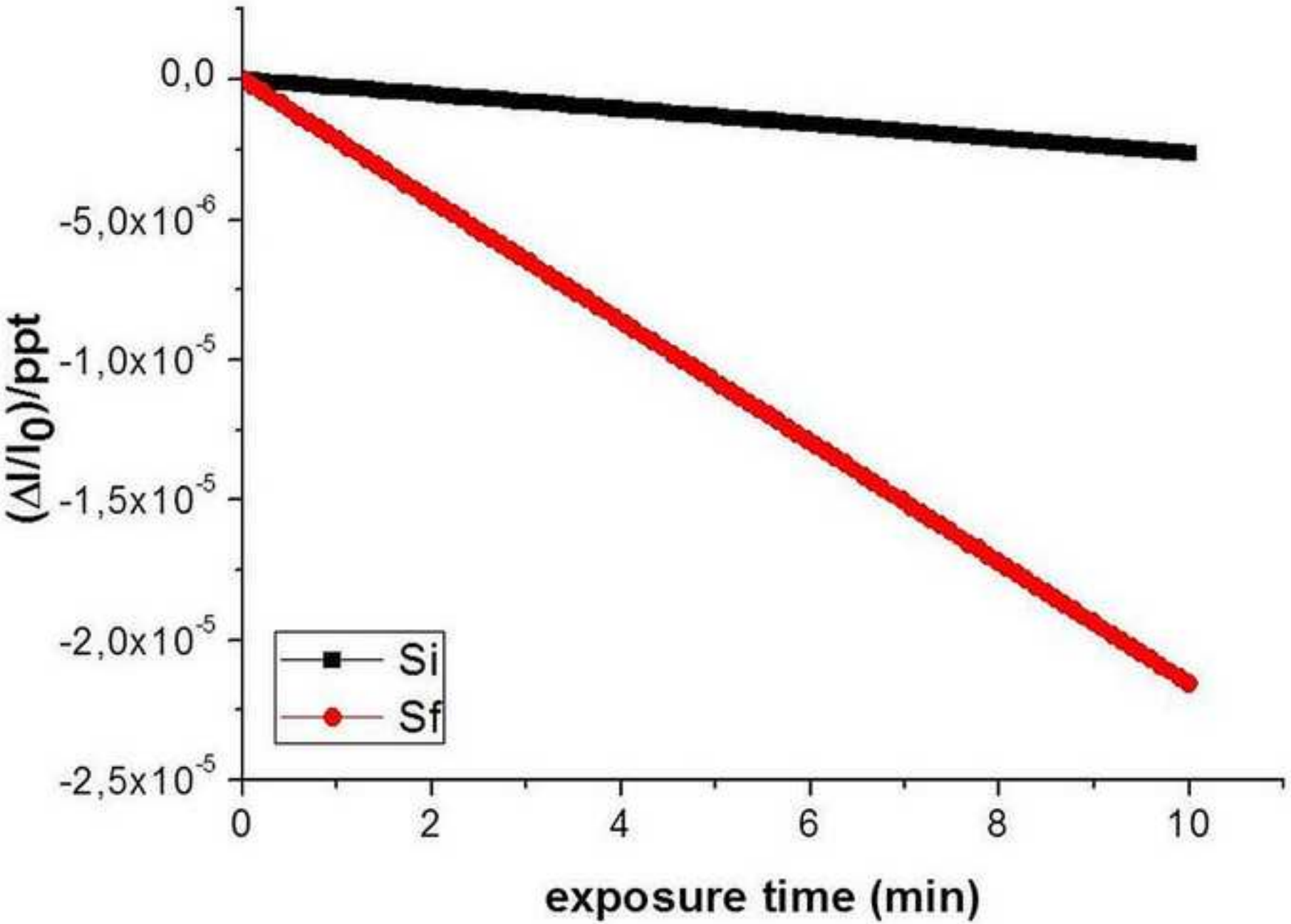

Figure(9)

Click here to download high resolution image

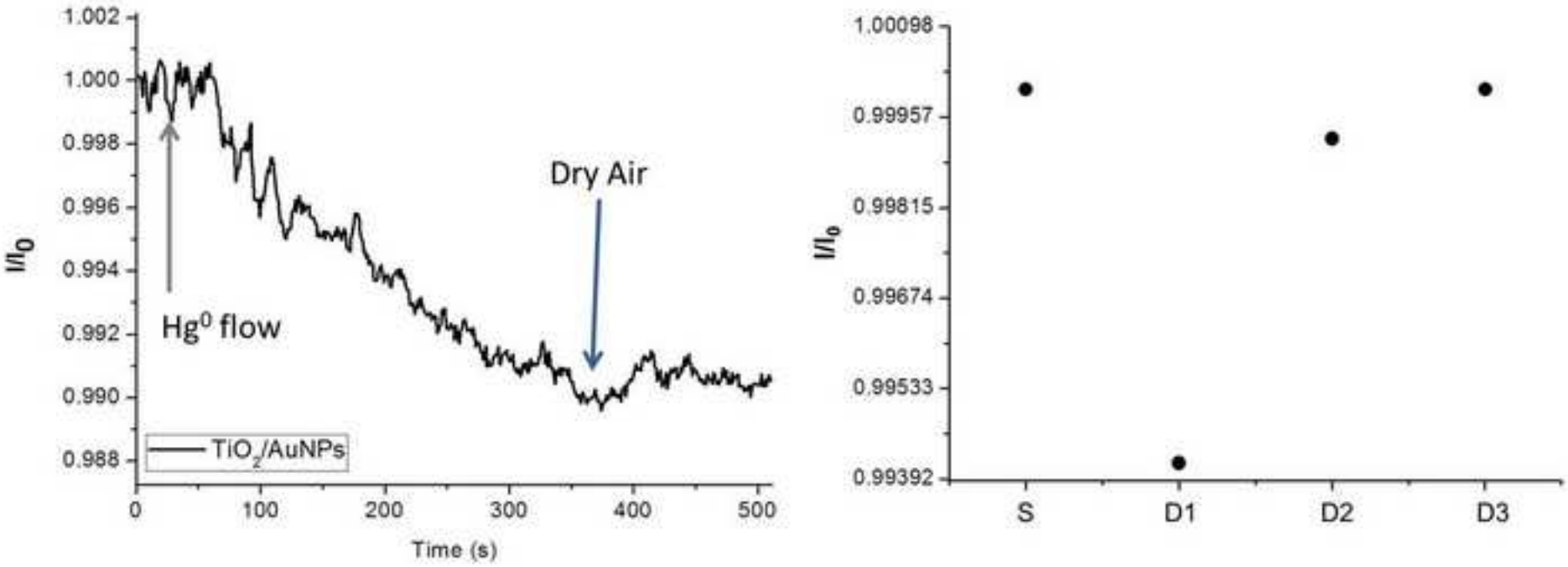

Figure(10)
Click here to download high resolution image

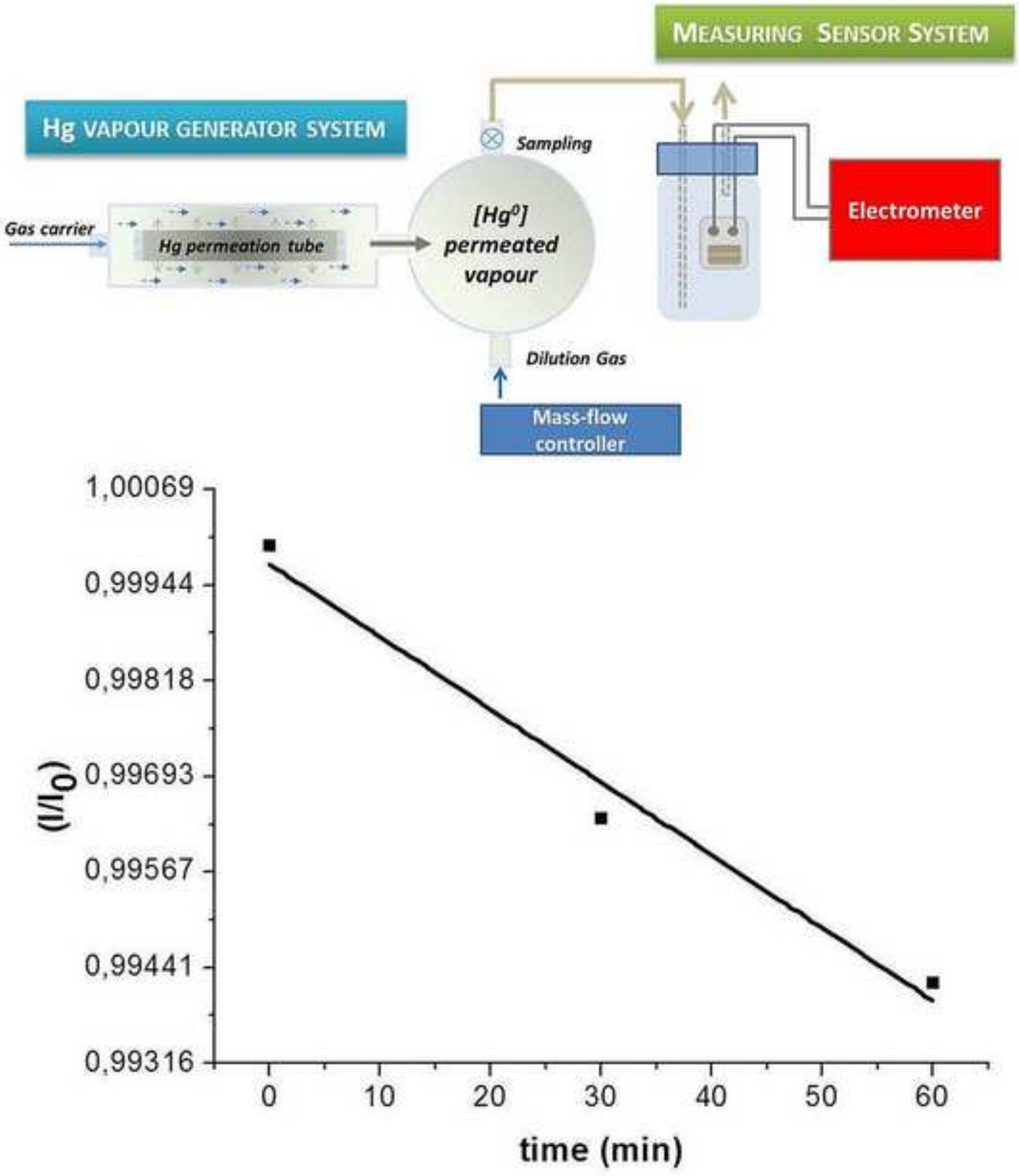

Author Biographies

Antonella Macagnano received the Biological Science's Degree in 1993 at Lecce University and the Professional's Degree in 1994. Since 2001 she is Research Scientist at the National Research Council (CNR). She has been leader (2001-2013) of the job-order entitled "Bio-inspired Sensoristic Systems and Technologies for Space and Human Safety" at Institute for Microelectronics and Microsystems (IMM) of CNR. Since 2013, she is Researcher and Leader of the action called "High-Performance Sensors and Sensing Systems for Monitoring Air Quality and Environment" at Institute of Atmospheric Pollutant Research (IIA) of CNR. She has been cooperating with many International and National scientists for designing and studying novel sensors (gravimetric, conductive, capacitive) and bio-inspired sensing strategies, based on nanostructured and bio-functionalized materials for environmental and biomedical applications, within several projects (among them, various as a leader). At present, she is member of the Management Committee of a European Cooperation in Science and Technology (COST) Action MP1206 entitled "Electrospun Nano-fibres for Bio-inspired Composite Materials and Innovative Industrial Applications" (2013-2017) and the leader of the Working Group devoted to Industrial/Technical applications.

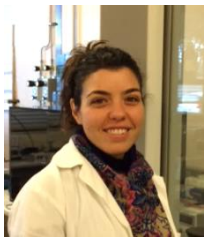

Viviana Perri received the Chemistry and Pharmaceutical Technology's degree in 2012. Currently she is carrying out her PhD studies at University of Calabria in Science and Technologies of Materials and her experimental work at Institute of Atmospheric Pollution Research of CNR. Her main research activity is focussing on the potentials of hybrid nanostructures for chemical sensors.

Emiliano Zampetti received a degree in Electrical Engineering in the 2002. In the 2007 he obtained a Ph. D degree in Electronic Engineering of sensorial and learning systems. Since 2014 he is research scientist at Institute of Atmospheric Pollution Research (IIA) of the National Research Council (CNR). His main research activities regard: design and development of high performances electronic interface circuits for sensory systems like to chemical sensor array and Electronic Nose; design and development of micro-transducers for sensors (e.g. IDE, micro capacitance) implemented on silicon and flexible substrate; study and characterization of materials for acoustic wave sensors (QCM, SAW), CHEM-FET and chemo-resistor; development of suitable equipment for electrospinning and electrospun for functionalized polymer materials to create nanofibers and

microstructures for nano-technological applications in the field of sensors and organic electronics. He has been cooperating within European Projects (FP7, ESA) and National Projects with International Universities, Research Institutes and SMEs.

Andrea Bearzotti received the Laurea degree in Physics from the University of Rome "La Sapienza" in February 27, 1986 with a thesis titled: "M.O.S. structure with palladium gate as hydrogen and oxygen sensor". Since 1988 he is Research Scientist at the National Research Council (CNR). His present interest is focused on the development of gas sensing systems based on nano- and meso-structured materials. He has been responsible of several National Projects and referee, in International Projects, for EC in FP5 (GROWTH) and FP6 (IST).

Fabrizio De Cesare received the degree in biology from the University of Rome La Sapienza, Rome, Italy, in 1989 and PhD in agricultural chemistry from University of Tuscia, Viterbo, Italy in 1994. Currently he is researcher with Faculty of Sciences of University Tuscia, Viterbo, Italy. His main research activities are concerned with the study of soil biochemistry and chemistry, ad–absorption phenomena, soil remediation, composting, phytopathogens biocontrol and sensor applications in environment.

Nicola Pirrone received the degree in Nuclear Engineering, University of Pisa (1989) and currently he is Adjunct Professor / SPH-EHS, University of Michigan, Ann Arbor, USA (2012 – present) and IIA-CNR Director (2008-present). During the last 20 years he had an active role in focussing different aspects related to biogeochemical cycles of atmospheric pollutants, atmospheric chemistry and air quality, global changes and development and implementation of environmental policies. Main of his activity is spent as expert member/chair /head of Italian delegations in European, International and National programs and task forces related to different aspects of Earth Observation, Environmental Research, Environmental Policy development and Evaluation of research strategies in EU and abroad.

Francesca Sprovieri received the degree in Geology and PhD in Engineering, University of Calabria. Her experimental activity, as scientific coordinator, is devoted to intensive measuring campaigns in urban, rural and remote, and the creation and implementation of new laboratory analytical techniques for the study of the main pollutants in the atmosphere and aquatic ecosystems with particular reference to air mercury.

Anna Maria Ferretti received her master in 1999 in Chemistry, her PhD (2002) in Chemical Sciences from the University of Milan. From 2003 to 2009 she was a temporary Research Scientist at the National Institute of Material Physics. From 2009 she got a permanent position as Research Scientist, at CNR at Institute of Molecular Science and Technologies (ISTM). Since she joined the ISTM, she focused her research activity on the synthesis and characterization of ferro-, antiferro-, and ferri-magnetic nanoparticles. She is also an expert in Transmission Electron Microscopy (TEM) and also in the analytical technique related (EELS, ESI, STEM/EDX).